

THERMAL-HYDRAULIC AND FUEL PERFORMANCE CODE COUPLING FOR MULTI-
PHYSICS INDUSTRIAL APPLICATIONS

A Thesis

by

KALEB TODD NEPTUNE

Submitted to the Office of Graduate and Professional Studies of
Texas A&M University
in partial fulfillment of the requirements for the degree of

MASTER OF SCIENCE

Chair of Committee,
Co-Chair of Committee,
Committee Member,
Head of Department,

Yassin A. Hassan
Rodolfo Vaghetto
Maria King
Yassin A. Hassan

August 2018

Major Subject: Nuclear Engineering

Copyright 2018 Kaleb Neptune

ABSTRACT

In order for the existing United States fleet of nuclear power plants to maintain an economic competitive edge, innovative technologies to extend the life of the plants and reduce the operational costs while maintaining energy demands must be implemented. The U.S. Nuclear Regulatory Commission (NRC) is currently proposing rulemaking 10 CFR 50.46c to revise the loss-of-coolant-accident (LOCA) and emergency core cooling system (ECCS) acceptance criteria to include the effects of higher burnup on cladding performance [1]. This proposition means that the core of the reactor, including the fuel and cladding, cannot be treated as an isolated system when performing safety evaluations. This calls for the means to develop multi-physics evaluation methods for Design Basis Accident (DBA) scenarios. Efforts are currently undergoing towards developing advanced predictive simulation packages that can more accurately represent the multi-physics aspects and uncertainties of a nuclear power plant behavior during normal operation and accident scenarios.

Remarkable efforts have been taken by Idaho National Laboratory (INL) to develop a multi-physics simulation package. Within the Light Water Reactor Sustainability (LWRS) program the Loss of coolant accident Toolkit for U.S. (LOTUS) has been developed, consisting of multiple codes to study the complex phenomena involved in light water reactor accident scenarios. The toolkit includes a specialized code for thermal-hydraulic system simulations (RELAP5-3D), a fuel performance behavioral analysis code (FRAPCON-4.0), a dynamic risk analysis code (RAVEN), and a core design optimization code (PHYSICS).

The objective of this thesis is to develop a coupling technique between RELAP5-3D and FRAPCON, and to determine if physical phenomena predicted by the stand-alone codes are

preserved. A demonstration run has been executed using plant-specific parameters representative of the South Texas Project (STP) nuclear power plant, to demonstrate the use of the coupled codes for industrial applications. A benchmark exercise is included in this research to verify the compatibility of FRAPCON and BISON using the same single pin model. The benchmark is used to confirm the applicability of the developed coupling technique to the new fuel performance code BISON. Simulation results from FRAPCON-4.0 and BISON confirmed applicability of the coupling methodology to each fuel performance code, by preserving fuel pins temperature profile and stored energy. The developed coupling technique contribute to the advancements of the toolkit to support industry applications.

ACKNOWLEDGEMENTS

I would like to express my sincere appreciation to my supervisors, Dr. Yassin Hassan, Dr. Rodolfo Vaghetto, and Co-worker Alessandro Vanni because their guidance made this work possible.

This project represented a unique opportunity for collaboration between Texas A&M University, Idaho National Laboratories and South Texas Project. I would like to personally thank Zhang Hongbin, Ronaldo Szilard, and Cole Blakey from INL for their constant support and mentoring which improved the quality of this study. I would also like to thank the engineers at South Texas Project for providing the crucial data needed to conduct the demonstration case.

My final gratitude goes to my parents, Kyla and Renee Villegas, Grandfather, Byron Grover, and friends, Selena Baiza and Adrian Campa, who provided the support and nourishment necessary to successfully complete this task.

CONTRIBUTORS AND FUNDING SOURCES

This work was supervised by a thesis committee consisting of Professors Yassin Hassan and Rodolfo Vaghetto of the Department of Nuclear Engineering and Professor Maria King of the Department of Mechanical Engineering.

All work for the thesis was completed by the student, under the advisement of Professors Yassin Hassan and Rodolfo Vaghetto of the Department of Nuclear Engineering.

The funds for this work were provided by INL through a project established between INL and Texas A&M University (DE-AC07-05ID14517)

NOMENCLATURE

1D	One - Dimensional
2D	Two - Dimensional
3D	Three - Dimensional
10 CFR 50.46c	Title 10, Code of Federal Regulations
ATF	Accident Tolerant Fuel
BWR	Boiling Water Reactor
DBA	Design Basis Accident
FTHCON	Fuel Thermal Conductivity model
INL	Idaho National Laboratory
LOCA	Loss Of Coolant Accident
LOTUS	Loss Of coolant accident Toolkit for U.S.
LWR	Light Water Reactor
LWRS	Light Water Reactor Sustainability program
MOX	Mixed Oxide fuel
NFI	Nuclear Fuel Industries
NRC	Nuclear Regulatory Committee
PNNL	Pacific Northwest National Laboratory
PWR	Pressurized Water Reactor
RELAP	Reactor Excursion and Leak Analysis Program
STP	South Texas Project
TRACE	TRAC/RELAP Advanced Computational Engine

UO₂

Uranium Dioxide

TABLE OF CONTENTS

	Page
ABSTRACT.....	ii
ACKNOWLEDGEMENTS	iv
CONTRIBUTORS AND FUNDING SOURCES	v
NOMENCLATURE	viii
TABLE OF CONTENTS.....	ix
LIST OF FIGURES	xiii
LIST OF TABLES	xiii
1 INTRODUCTION	1
1.1 LOCA Toolkit for U.S. (LOTUS)	3
2 MOTIVATION AND OBJECTIVES.....	5
2.1 Objectives	6
2.2 Stored Energy	7
3 SYSTEM CODE DESCRIPTION	8
3.1 RELAP5-3D.....	9
4 FUEL PERFORMANCE CODE DESCRIPTION	11
4.1 FRAPCON-4.0.....	12
4.2 BISON	12
5 FRAPCON-4.0 AND RELAP5-3D MODEL DEVELOPMENT	14
5.1 FRAPCON-4.0 Model Development.....	14
5.2 RELAP5-3D Model Development.....	17

5.3	Material Properties Description	22
5.3.1	Fuel Thermal Conductivity	22
5.3.2	Gap Conductance Models	25
6	FRAPCON-4.0 AND RELAP5-3D SIMULATION RESULTS	31
6.1	Preliminary RELAP5-3D Model Simulation Results	31
6.2	Final RELAP5-3D Model Simulation Results.....	34
7	BISON AND FRAPCON-4.0 MODEL DEVELOPMENT	38
7.1	BISON Model Development	38
7.2	FRAPCON-4.0 Model Development.....	45
7.3	Material Properties Description	47
7.3.1	Fuel Thermal Conductivity	47
7.3.2	Gap Conductance	48
8	BISON AND FRAPCON-4.0 SIMULATION RESULTS	51
9	CONCLUSION.....	54
	REFERENCES	56

LIST OF FIGURES

Figure 1.1 Illustration of the LOTUS Framework Reprinted from [2]	4
Figure 5.1: Time-Dependent Average Linear Heat Generation.....	16
Figure 5.2: Time-Dependent Axial Power Profiles	16
Figure 5.3: FRAPCON-4.0 Model Radial Power Profiles.....	17
Figure 5.4: RELAP5-3D Single Pin Nodalization Diagram.....	18
Figure 5.5: RELAP5-3D Model Axial Power Profile.....	20
Figure 5.6: RELAP5-3D Model Averaged Radial Power Profile.....	21
Figure 5.7: Axial Dependent Burnup at Last Time-Step of FRAPCON-4.0 Simulation.	24
Figure 5.8: Segmentation of the gap in the RELAP5-3D dynamic gap conductance model.....	26
Figure 6.1: Radial temperature profile of the initial model at the center axial node.	32
Figure 6.2: Center axial node radial temperature profile simulation results of refined system code model with modified fuel thermal conductivity properties.	33
Figure 6.3: Center axial node radial temperature profile simulation results of refined system code model with averaged radial power profile.	34
Figure 6.4: FRAPCON-4.0 and RELAP5-3D comparison results of radial temperature profiles at the first axial node.	35
Figure 6.5: FRAPCON-4.0 and RELAP5-3D comparison results of radial temperature profiles at the seventh axial node.	36
Figure 6.6: FRAPCON-4.0 and RELAP5-3D comparison results of radial temperature profiles at the fifteenth axial node.	36
Figure 7.1: Fuel Rod Physical Model Diagram [18].....	40
Figure 7.2: Time Dependent Axial Power Profiles.....	41
Figure 7.3: Time-Dependent Coolant Inlet Temperature	42
Figure 7.4: Time-Dependent Coolant Inlet Pressure	43
Figure 7.5: Time-Dependent Average Linear Heat Generation Rate	44
Figure 7.6: Time-dependent fast neutron flux	45

Figure 8.1: BISON and FRAPCON-4.0 model radial temperature profiles comparison near bottom of fuel pin.	51
Figure 8.2: BISON and FRAPCON-4.0 model radial temperature profiles comparison in the middle of fuel pin.	52
Figure 8.3: BISON and FRAPCON-4.0 model radial temperature profiles comparison near top of fuel pin.	52

LIST OF TABLES

Table 4.1: FRAPCON-4.0 Model Main Parameters (Based on STP plant data).....	15
Table 4.2: FRAPCON-4.0 Model Parameters Used in the RELAP5-3D Model.....	19
Table 4.3: Fuel Thermal Conductivity table used in RELAP5-3D model.....	25
Table 4.4: FRAPCON-4.0 and Relap5-3D Gap Conductance Model Breakdown of Gas Conductance [6] [15].....	28
Table 5.1: Stored energy comparison between the RELAP5-3D model and FRAPCON-4.0 model.	37
Table 6.1: General BISON Model Parameters	39
Table 6.2: FRAPCON-4.0 general parameters used to build a single pin model.	46
Table 6.3: FRAPCON-4.0 and BISON Gap Conductance Model Comparison [22] [12].....	48

1 INTRODUCTION

To remain competitive in the energy market, the nuclear industry must find ways to improve reactor systems to operate more efficiently. Optimization of a reactor system requires a deep knowledge of the behavior of the reactor environment. The complexity of the system poses a challenge when developing methods for plant life extension. One of the largest design limitations of a nuclear system is the temperature of the fuel cladding. To maintain safe operation under transient conditions, the behavior of the system must be understood. Advancements in computing capabilities has led to the development of models to perform complex calculations of multi-physical phenomena to accurately predict the behavior of the system during these transient conditions.

Specialized codes have been developed to simulate specific aspects of the complex multi-physical environment experienced in a reactor system. For example, there are system codes that effectively represent the thermal-hydraulic behavior of a power plant during both steady-state and transient conditions. Some of these advanced thermal-hydraulic codes have the capability to perform simple fuel performance calculations such as rupture models and ballooning. These system codes are still limited in their ability to perform detailed analysis of the fuel behavior such as fission gas released, rod internal pressure, and fuel/cladding mechanical interactions [2]. Some limitations also exist for fuel performance codes. Fuel performance codes were developed to perform detailed analysis of the behavior of a single pin in a reactor core. For a fuel performance code to accurately perform behavioral analysis the time-dependent surrounding conditions must be supplied to the code. The simulation capabilities of these specialized codes

can be improved if data was easily exchanged between them. The need to enhance these computational behavior simulations motivates the development of a couple between codes.

1.1 LOCA Toolkit for U.S. (LOTUS)

A multi-physics simulation package is being developed by Idaho National Laboratories (INL), under the Light Water Reactor Sustainability (LWRS) program lead by the Department of Energy (DOE). This program has created the Loss of coolant accident Toolkit for U.S. (LOTUS) that covers five technical disciplines. Specialized codes simulate each of the five disciplines and communicate data between each other to simulate transient conditions such as LOCA scenarios. The LOTUS package currently uses the codes listed in Table 1.1 to perform transient calculations. Eventually LOTUS will move towards using the advanced specialized codes listed in the last column of Table 1.1 to perform more detailed LOCA analysis.

Table 1.1: LOTUS Codes [4]

Disciplines	Current Codes used by LOTUS	Future Codes for use in LOTUS
Core Design (CD-A)	HELIOS-2	HELIOS-2
Fuel Performance (FP)	FRAPCON-4.0/FRAPTRAN	BISON
Reactor Thermal-Hydraulics and System Analysis (SA)	RELAP5-3D	RELAP7
Risk Assessments (RA)	RAVEN	RAVEN
Core Design Optimization (CD-O)	PHYSICS	VERA-CS

Figure 1.1 provides an illustration of how each specialized code works within the LOTUS framework.

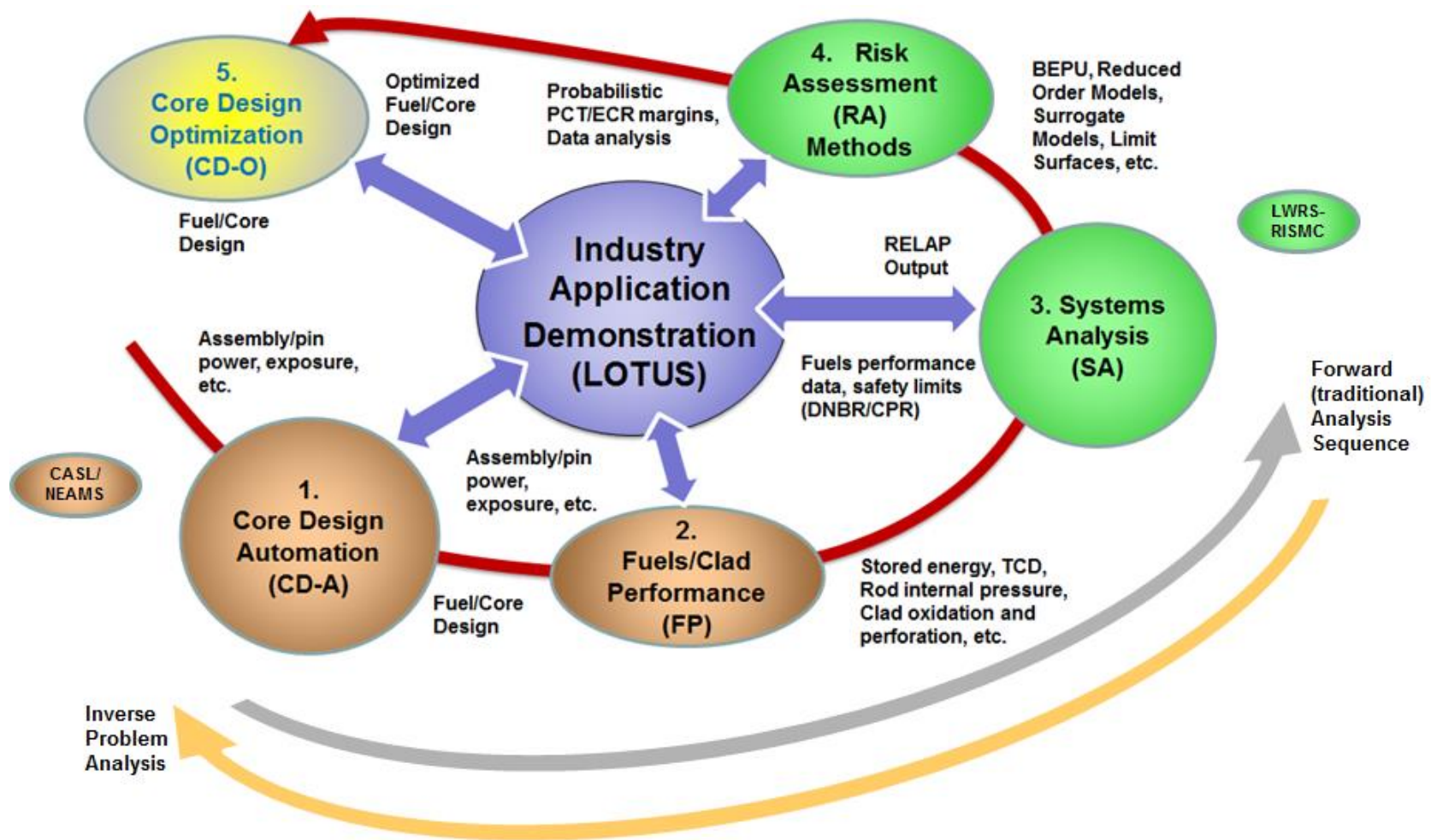


Figure 1.1 Illustration of the LOTUS Framework Reprinted from [2]

2 MOTIVATION AND OBJECTIVES

The LOTUS package is being developed to allow plant owners the ability to perform multi-physics calculations of complex nuclear systems. The goal of LOTUS is to provide simulation capabilities that enables the plant owner to better understand the behavior of the plant in a LOCA. These calculations allow the plant owner/operators to make decisions of how to maintain the safety of the plant and meet regulatory requirements. LOCA analysis performed in the LOTUS framework requires initial conditions to be supplied to the system analysis module from the fuel performance module. The initial conditions required by the thermal-hydraulic system analysis code, RELAP5-3D, can be supplied directly to the simulation model from any fuel performance code through a couple. The couple allows the automation of system analysis based off fuel performance results.

2.1 Objectives

Establishing a proper couple between a system code and a fuel performance code is a process that requires certain steps to be achieved. The goal is to achieve each listed step in their respective order:

1. Establish a single rod reference model.
2. Develop another model in the alternate code based of the reference model.
3. Satisfy physical phenomena between simulation results of each code.

A couple between the current fuel performance code in the LOTUS framework, FRAPCON-4.0, and the system code, RELAP5-3D, will be established by setting a FRAPCON-4.0 model as the reference. This model will be based of STP plant parameters and will provide the essential data needed to build a RELAP5-3D model. Once each model is fully developed simulation results will be analyzed to ensure physical phenomena is preserved.

Once the coupled fuel performance code model and system code model is complete then an exercise can be performed to determine if a BISON fuel performances code model can be used in place of a FRAPCON-4.0 code model. The same list of steps required to make the couple between the system code and fuel performance code are required to determine if the new fuel performance code is applicable to the LOTUS framework. A BISON single pin model based of typical PWR plant parameters will be established as the reference model for the benchmark. This single pin model will be used to build another model in FRAPCON-4.0 based off the same parameters. The simulation results of each of the code model will determine if the same input parameters yield the same simulation results between each fuel performance code model.

2.2 Stored Energy

When coupling two or more codes it is important to ensure that physical phenomena are preserved. Preservation of physical phenomena is achieved when the general parameters that overlap between code simulations are consistent. When performing LOCA simulations the important parameter that must be conserved between a fuel performance code and a system code is the energy stored in the fuel. In a LOCA scenario the stored energy calculated by the fuel performance code is related to the Peak Cladding Temperature (PCT) which sets the transient conditions for the thermal-hydraulic system analysis. This parameter depends on the radial temperature profile of the fuel, which is calculated by both codes. Other parameters that contribute to the radial temperature profile of the fuel must also be analyzed to ensure the stored energy is preserved. The codes thermal properties play a large role in how the radial temperature profile is created. Detailed analysis of each codes method for determining the thermal conductivity, specific heat capacity and gap conductance must be performed. It is equally important to ensure the same amount of power is being supplied to each code's model.

The stored energy is calculated by summing the energy of each pellet ring calculated at the ring temperature [3]. The expression for stored energy is:

$$E_s = \frac{\sum_{i=1}^I m_i \int_{298K}^{T_i} C_p(T) dT}{m} \quad (1.1)$$

In Equation 1.1 m_i is mass of ring segment i , T_i is temperature of ring segment i , $C_p(T)$ is specific heat evaluated at temperature T , m is total mass of the axial node, and I is the number of annular rings.

3 SYSTEM CODE DESCRIPTION

Since modern nuclear reactors are highly complex systems that consist of multiple physical aspects spanning across different theoretical models, there is a need to develop tools in order to better understand the systems behavior as a whole. There has been an extensive amount of work over the last 30 years towards developing advanced computational tools to simulate the thermal-hydraulic behavior of complex reactor systems during steady-state, and transient conditions, with a particular interest on simulations of loss of coolant accident scenarios and other design basis accidents [5]. These simulations are important for making critical decisions when designing and operating nuclear power plants. An international agreement between countries has helped the development of these system codes. The collaboration between the NRC, power utilities, and foreign countries provides a large range of application, which results in accelerated system code improvements and error corrections [4].

Several specialized system codes have been developed for analysis of the reactor system and containment response during transient scenarios. TRACE (TRAC/RELAP Advanced Computational Engine) and RELAP5 (Reactor Excursion and Leak Analysis Program) are most used system codes that are capable of simulating large and small LOCA and other transient for both PWRs and BWRs. The original TRACE code series was developed to perform 2-D simulations and updated to include TRAC-P and TRAC-B. TRAC-P can perform 1-D, 2-D, or 3-D simulations of large break LOCA analysis in PWRs and TRAC-B can perform 1-D, 2-D, or 3-D simulations of large break LOCA analysis in BWRs. The RELAP5 is a series of system codes designed to perform LWR reactor transient analysis. A number of system codes have been also

developed to simulate the reactor containment response during transient scenarios. MELCOR, CONTAIN, and GOTHIC are the most used among the containment analysis tools.

3.1 RELAP5-3D

The RELAP5-3D is the system code currently in use in the multi-physics toolkit LOTUS. The code belongs to the well-known RELAP5 family of system codes that was designed and largely used for analysis of LWRs [4].

The RELAP5 code series has been developed to perform many transient simulations, such as, loss of coolant accident scenarios and an anticipated transient without scram. The code series has also included simulation of operational transients such as loss of offsite power, station blackouts, and loss of feed water scenarios [5]. The latest code in the RELAP5 series is RELAP5-3D which is a highly generic code that can not only calculate the behavior of the reactor coolant during a transient scenario but it can also be used for simulations of a wide variety of thermal-hydraulic transient simulations not only for nuclear applications [6].

The RELAP5-3D code is a successor to the RELAP5/MOD3 code which was developed for the Nuclear Regulatory Commission [7]. There are many improvements made to the RELAP5-3D code which enhances it over its predecessors. The most prominent improvement is the fully integrated, multi-dimensional thermal-hydraulic modeling capabilities [7]. This improvement allows the code to be applied to many postulated reactor accident scenarios. The RELAP5-3D code includes new thermal dynamic properties and a new matrix solver which make the code more robust. The RELAP5-3D multi-dimensional component allows any component or region of a LWR system be more accurately modeled [6]. The RELAP5-3D code was adopted by INL for the LOTUS framework because of its past extensive use analysis of

LOCA scenarios and other LWR transients. The RELAP5-3D was also developed at INL, allowing for direct collaboration with the system code's developers when needed.

4 FUEL PERFORMANCE CODE DESCRIPTION

When performing safety analysis of a nuclear reactor it is important to be able to accurately predict the behavior of the fuel. Fuel performance codes are developed to model fuel behavior in both steady-state and transient conditions. Fuel performance simulation help broaden our understanding of fuel behavior which leads to decisions for operation conditions of existing plants, and design considerations for new nuclear reactor [4]. Since there is a constant demand for improving the reactor fuel efficiency, maintaining adequate safety margins, fuel performance codes are also used in the development of new fuels, such as Accident Tolerant Fuel (ATF). Fuel performance codes have developed capabilities to properly analyze the thermal and mechanical performance of the fuel in nuclear reactor systems [8]. Phenomena of interest that can be simulated with fuel performance codes include the fuel densification, fuel and cladding swelling, fission gas generation, fission gas release, and irradiation damage of the fuel. Fuel performance codes can be classified as either transient or steady state codes [5].

One of the main uses of steady-state simulation codes is to provide result including the stored energy for LOCA analysis. Single-rod codes developed for steady-state simulations, such as, FRAPCON, calculate the thermal and mechanical parameters of interest including creep down, irradiation growth and fission gas released to the gap [3].

Single-rod codes developed for transient, such as, FRAPTRAN, perform mechanical and thermal analyses of the fuel under transient conditions [8]. The differences between a steady-state and transient fuel performance codes are that transient codes do not include long-term phenomena like creep and use transient heat transfer terms in their solutions.

4.1 FRAPCON-4.0

FRAPCON-4.0 has been developed for the NRC by Pacific Northwest National Laboratory (PNNL) to calculate the steady-state behavior of high burnup fuel. The code uses a finite difference heat conduction model based on a variable mesh spacing, to account for the peaking power towards the outer edge of the fuel pellet for high-burnup fuels [9]. FRAPCON-4.0 also uses a single channel coolant enthalpy rise model, and has been validated for analyses of BWRs, PWRs and heavy-water reactors. FRAPCON-4.0 was adopted by INL for use in the LOTUS framework since it has been used extensively in the past for steady-state simulations of LOCA scenarios and because the fuel performance code BISON shares many of the same solution correlations.

4.2 BISON

BISON is a fuel performance code that is capable of finite element analysis of nuclear fuel under steady-state and transient conditions [10]. BISON is being developed by INL under the MOOSE framework, enabling the code to efficiently solve problems on very large high-performance computers. BISON also has the capability to perform fuel performance analysis on new fuel types under development [11]. The code solves a fully-coupled set of equations for thermal and mechanic phenomena occurring within the fuel. It includes capabilities to simulate fuel behavior for either 1D spherical, 2D axisymmetric, or 3D fuel geometries.

There are important models and correlations that must be analyzed when comparing simulation results obtained by fuel performance codes, particularly the ones adopted to calculate

material properties such as thermal conductivity and gap conductance. Models of interest to the present work will be analyzed and compared for both the FRAPCON-4.0 and BISON codes.

5 FRAPCON-4.0 AND RELAP5-3D MODEL DEVELOPMENT

This section describes the development of the FRAPCON-4.0 fuel performance code model and the RELAP5-3D system code model. To ensure consistency between the predictions of the fuel performance code and system code, the RELAP5-3D model representing a single fuel pin model based off the reference FRAPCON-4.0 model. This single pin FRAPCON-4.0 model is prepared using plant characteristic data of the South Texas Project nuclear power plant. This model will serve as the primary reference for the preparation and simulation results of a RELAP5-3D single pin model.

5.1 FRAPCON-4.0 Model Development

The FRAPCON-4.0 model is prepared to simulate the behavior of a fuel pin through two fuel cycles. The main parameters implemented into the model are listed in Table 5.1. Due to fabrication tolerances and other operational needs, the cladding inner diameter is typically larger than the fuel pellets outer diameter, creating a gap between the fuel pellet and the cladding. For a fresh fuel pin, this gap is initially filled with helium allowing for fuel swelling during operation. Thermal analysis is based off the behavior of the fuel, gap, and cladding material that make up the fuel rod. Axial and radial discretization of the geometry has been defined and implemented in the model.

Table 5.1: FRAPCON-4.0 Model Main Parameters (Based on STP plant data¹)

Parameter	Value Used in Model
Cold Plenum Length	7.0 inches
Cladding Thickness	0.02248 inches
Gap Thickness	0.003307 inches
Cladding Outer Diameter	0.374 inches
Fuel Rod Pitch	0.496 inches
Inner Pellet Radius	0.0 inches
Fuel Density	95% of Theoretical Density (10.96 gm/cm ³)
Initial Fill Gas Pressure	480 psia
Fuel Pellet Height	0.387 inches
Cladding Type	ZIRLO
Initial Fill Gas Type	Helium
Total Fuel Length	14 feet
Cladding Roughness	2.54E-04
Fuel Roughness	2.54E-04
Coolant System Pressure	2275.64 psia
Coolant Input Temperature	548.33°F
Mass Flux of Coolant	2.60E+06 lb/hr-ft ²
Fuel Enrichment	4.2%

The pin was subdivided into 15 axial nodes. The number of nodes was optimized to allow the implementation of different axial power profiles with reasonable spatial resolution. Different power profiles are supplied to the FRAPCON-4.0 model as a function of time. The simulation was executed through 54 time steps with varying increments, to cover a simulation period of 54 months. Figure 5.1 shows the average linear heat generation as a function of time implemented into the model. The axial power profile supplied to the model at three selected time steps are shown in Figure 5.2.

¹ All data included in the table and used in the models are publicly available

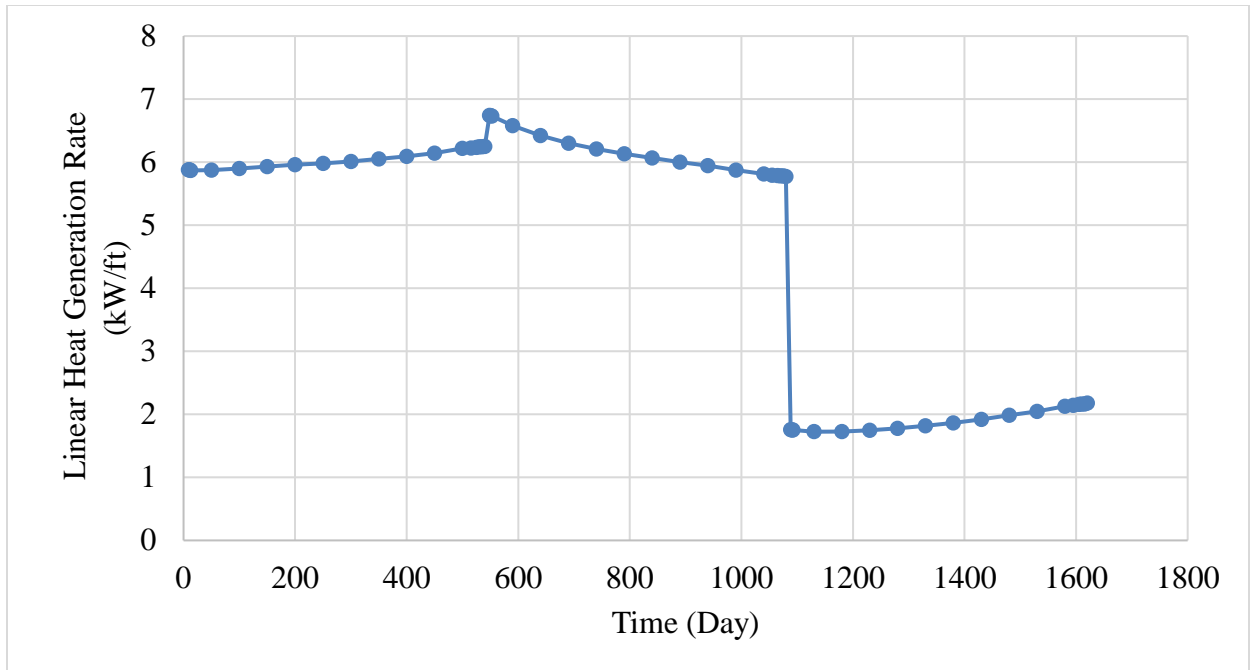


Figure 5.1: Time-Dependent Average Linear Heat Generation

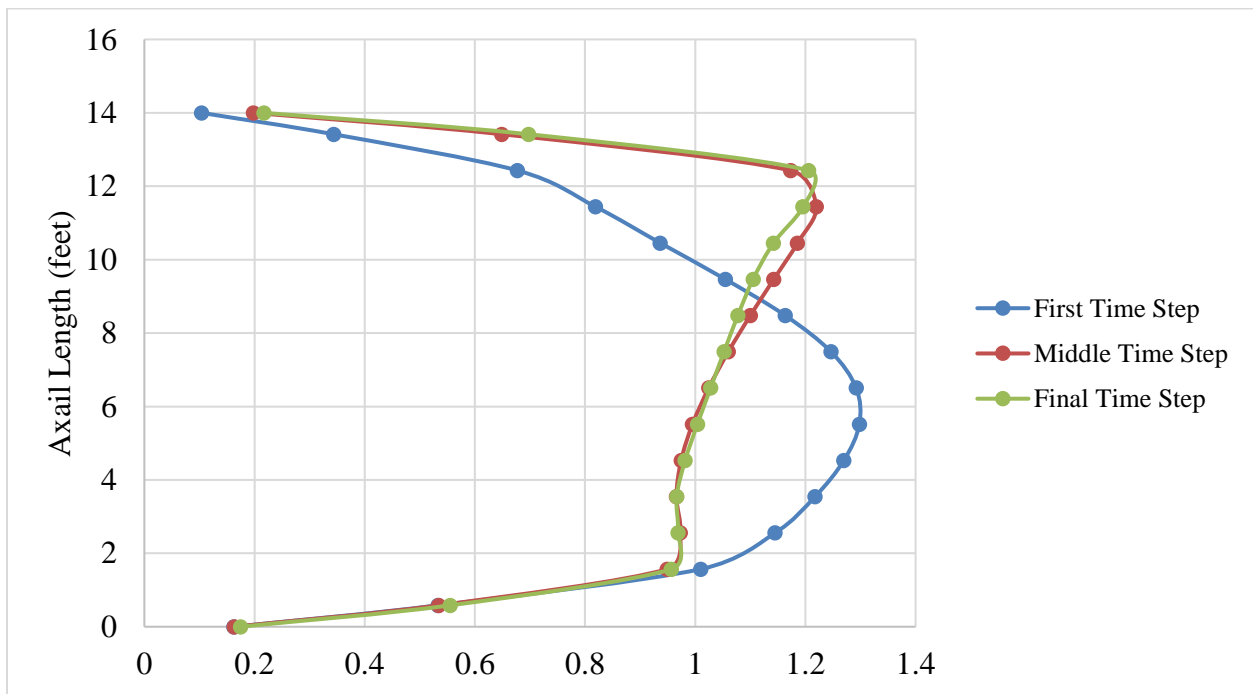


Figure 5.2: Time-Dependent Axial Power Profiles

Radial discretization has also been optimized to provide desirable spatial resolution of temperature and power profiles. The radial boundaries of the fuel pellet are automatically spaced

by the code with greater fraction in the outer region to optimize the heat generation radial distribution through the pin. Seventeen radial segments have been included to simulate the fuel region of the pin. Figure 5.3 shows the radial power distributions at three axial locations on the first time step.

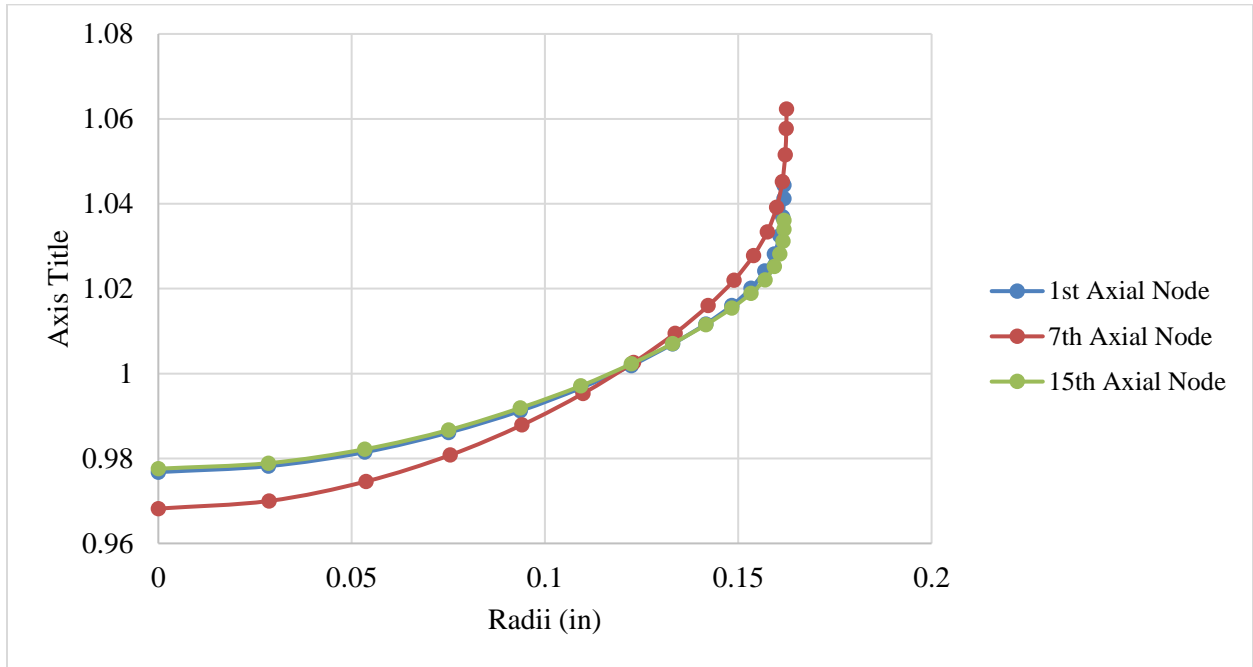


Figure 5.3: FRAPCON-4.0 Model Radial Power Profiles

5.2 RELAP5-3D Model Development

In order to simplify the comparison between the predictions of RELAP5-3D and FRAPCON-4.0, modeling technique including the spatial discretization approach adopted in the two codes were aligned. The same number axial and radial nodes defined in the FRAPCON-4.0 model are imposed to the RELAP5-3D model. The nodalization diagram adopted for the RELAP5-3D model is shown in Figure 5.4. The hydrodynamic model consists of a time-dependent volume to simulate the inlet boundary conditions, a vertical pipe component with 15 axial nodes, and a time-dependent volume to simulate the discharge ambient. As previously

mentioned, the time-dependent volume at the bottom of the diagram provides the inlet conditions of the coolant such as temperature and pressure. The pipe component simulates the flow channel surrounding the fuel rod. Junctions are defined to connect the components described above. A time-dependent junction is used to impose the desired channel flow rate. The fuel rod is simulated using a heat structure consisting of fifteen axial nodes with symmetric boundaries on the left side and convective boundaries on the right side (pipe component). Each of the forty-nine axial nodes are supplied data from the connected heat structure shown in Figure 5.4.

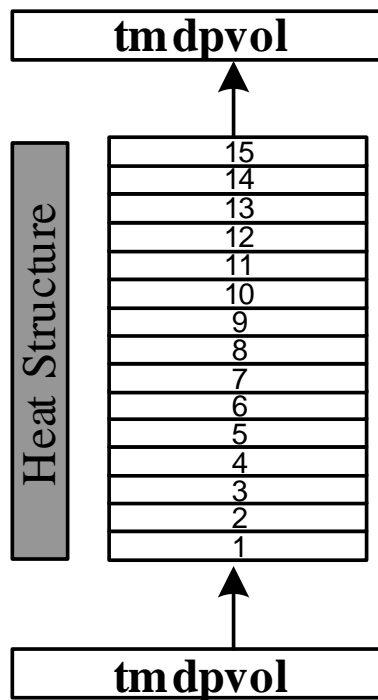


Figure 5.4: RELAP5-3D Single Pin Nodalization Diagram

The main parameters implemented in the RELAP5-3D model are the same of the ones defined for the FRAPCON-4.0 model and listed in. Table 5.2 defines the use of the FRAPCON-4.0 model parameters in the RELAP5-3D model.

Table 5.2: FRAPCON-4.0 Model Parameters Used in the RELAP5-3D Model

FRAPCON-4.0 Parameter	Value	RELAP5-3D Application
Nodal z-location	-	Provides the height of each node
Cladding thickness	0.2248 inches	Provides radial boundary for the cladding material
Pellet outer diameter	0.1613 inches	Provides radial boundary for the fuel material
Fuel/Clad Gap Width	0.003307 inches	Provides radial boundary for the gap material
Coolant Pressure	2275.64 psia	Provides pressure applied to nodes
Coolant Temperature	548.33°F	Provides coolant temperature applied to nodes
Rod Pitch	0.496 inches	Used to calculate the area of the flow channel
Fuel Roughness	2.54E-04	Supplied to the heat structure for each axial node
Cladding Roughness	2.54E-04	Supplied to the heat structure for each axial node
Cladding Outer Diameter	0.374 inches	Used to calculate the area of the flow channel
Inner Pellet Radius	0.0 inches	Sets the inside boundary for fuel radial segments
Fuel Density	95% of TD	Used in fuel thermal conductivity calculation
Initial Fill Gas Pressure	480 psia	Supplied to the heat structure
Cladding Type	ZIRLO	Used in fuel cladding conductivity calculation
Total Fuel Length	14 feet	Used to define axial geometric features
Mass Flux of Coolant	2.60E+06 lb/hr-ft ²	Used for coolant inlet velocity calculation

Since it is important to preserve the physical phenomena of fuel performance simulation in the system code simulation the final time step of the fuel performance simulation is used as the reference for the system code model construction. The time-dependent variable supplied to the system code model are listed below:

- Axial Power Profile
- Radial Power Profile
- Fuel Thermal Conductivity

The axial power profile implemented into the RELAP5-3D model is the one specified in the FRAPCON-4.0 model for the last time-step (Figure 5.5).

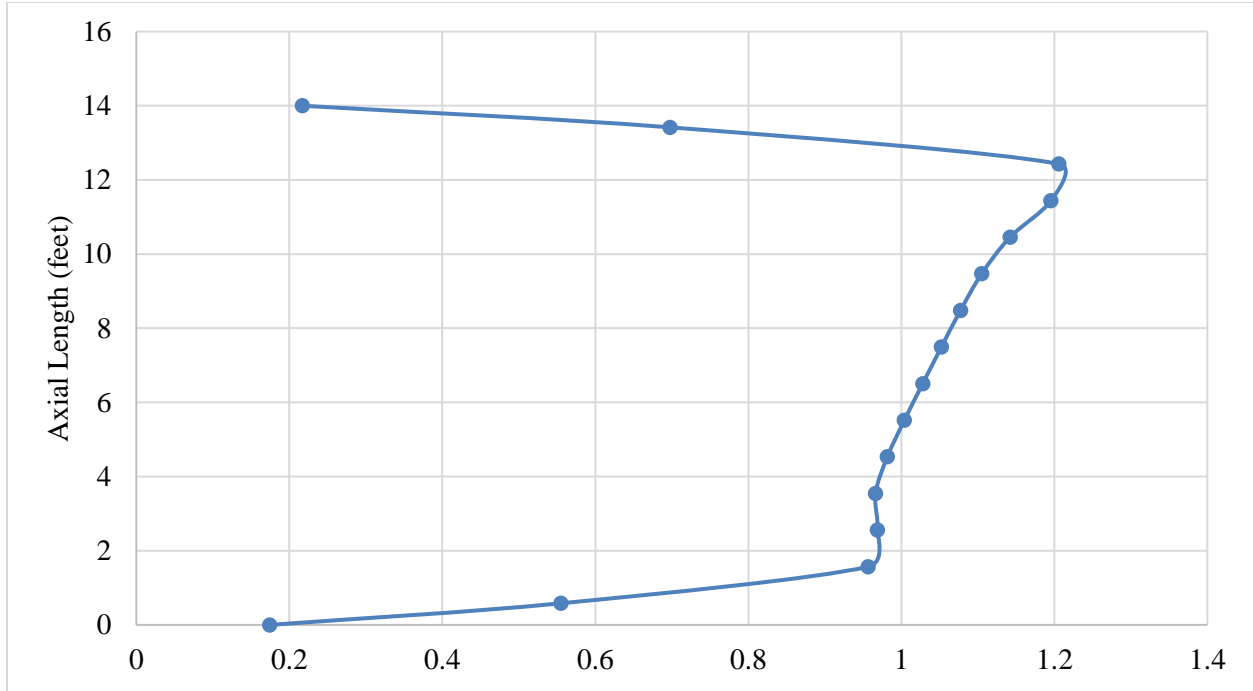


Figure 5.5: RELAP5-3D Model Axial Power Profile

As previously mentioned, the radial power profile in a fuel pin varies with axial location. When modeling the fuel pin in RELAP5-3D, certain limitations need to be accounted for. When a heat structure is defined with multiple axial nodes, the nodes may not be treated individually. In particular, a common radial power profile must be imposed to all axial nodes. To overcome this limitation, the spatial averaged radial power profile was implemented in the model and applied to each radial segment within the fuel. The radial segments also varied axially so an averaged value was obtained for the profile. The radial power profile generated from these averaged values is shown in Figure 5.6.

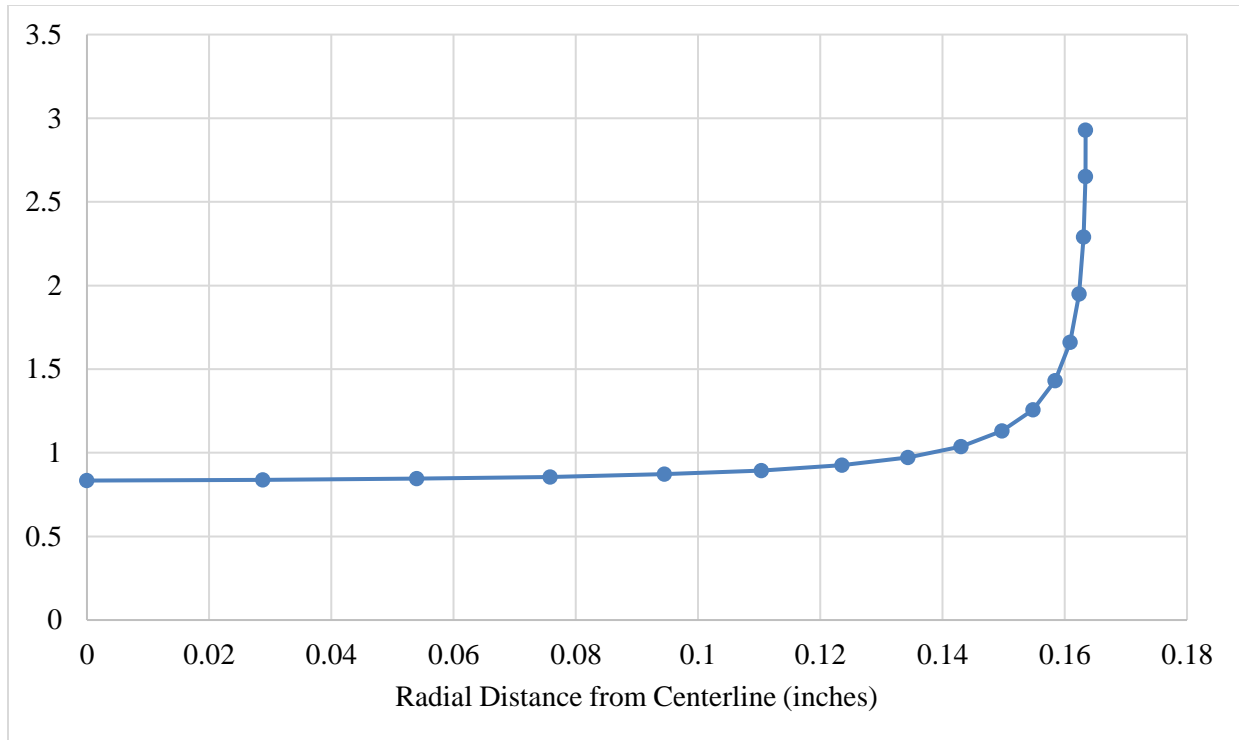


Figure 5.6: RELAP5-3D Model Averaged Radial Power Profile

RELAP5-3D requires thermal properties of the materials for fuel and cladding. These properties were extracted from the FRAPCON-4.0 theory manual and implemented into the RELAP5-3D in table format. Material properties required by the RELAP5-3D code are the thermal conductivity and specific heat capacity of the fuel, cladding, and gap. The thermal conductivity and specific heat capacity of the fuel and cladding are supplied to the system code in the form of user defined temperature dependent tables. In regards to the gap treatment, the dynamic gap conductance model has been enabled. This model calculated the gap conductance based on user-defined initial conditions. The detailed description of each model provided by the codes theory manuals will be covered in the next section.

5.3 Material Properties Description

Thermal properties for five materials are stored within the RELAP5-3D code. These materials include the gap, carbon steel, stainless steel, uranium dioxide, and zircaloy. These stored (built-in) properties can only be used if the conditions of the user's simulation case are satisfied by the property correlations. To better match the fuel thermal properties of FRAPCON-4.0 a table will be supplied to the RELAP5-3D model instead of using the stored uranium oxide properties in the system code. The fuel thermal properties will be generated from the FRAPCON-4.0 theory manual model description. Since the use of the dynamic gap conductance model is desired to enable simulations of transient conditions the built-in gap properties will also not be used in the RELAP5-3D model.

5.3.1 Fuel Thermal Conductivity

The Fuel Thermal Conductivity (FTHCON) model is used to calculate the thermal conductivity of the fuel pellet in the FRAPCON-4.0 code. Since the fuel pin's behavior is strongly dependent on the temperature, an accurate calculation of the thermal conductivity is critical. Thermal conductivity models used in FTHCON are functions of temperature, density, and burnup. The calculation of the fuel thermal conductivity has evolved from an original MATPRO model to the currently used modified Nuclear Fuel Industries (NFI) model [12]. The original MATPRO model is based on a mechanistic description of the thermal conductivity including lattice vibration and electron-hole pair contributions [13]. The basic theory behind the model is that the thermal conductivity can be represented as the sum of a lattice vibration, k_{phonon} and an electronic term, $k_{\text{electronic}}$, at 95% of its theoretical density. The k_{phonon} term is

typically inversely proportional to the sum of the temperature and the burnup dependent functions, while the $k_{\text{electronic}}$ term is usually an exponential function of inverse temperature.

$$k_{95} = k_{\text{phonon}} + k_{\text{electronic}} \quad (5.3.2)$$

The MATPRO model does not account for the degradation of the thermal conductivity with increasing burnup which is way it was replaced by the modified NFI model in the FRAPCON-4.0 code. The modified NFI model is based off an equation proposed by Ohira and Itagakia [13] [14], which calculates the thermal conductivity for 95% theoretical density in the following equation.

$$k_{95} = \frac{1}{A + BT + f(\text{Bu}) + (1 - 0.9 * \exp(-0.04 * \text{Bu}))g(\text{Bu})h(T)} + \frac{E}{T^2} \exp(-F/T) \quad (5.3.3)$$

Where,

K_{95} = thermal conductivity for 95% theoretical density

T = temperature, K

Bu = burnup, GWd/MTU

$f(\text{Bu})$ = effect of fission products in crystal matrix = $0.00187 * \text{Bu}$

$g(\text{Bu})$ = effect of irradiation defects = $0.038 * \text{Bu}^{0.28}$

$h(T)$ = temperature dependence of annealing on irradiation defects = $\frac{1}{1 + 369\exp(-Q/T)}$

Q = temperature dependent parameter (Q/R) = 6380K

A = $0.0452 \text{ m} * \text{K/W}$

$$B = 2.46 \times 10^{-4} \text{ m} \cdot \text{K/W}$$

$$E = 3.5 \times 10^9 \text{ W} \cdot \text{K/m}$$

$$F = 16361\text{K}$$

The modified NFI model described in Equation 5.3.3 was used to generate the thermal conductivities of the fuel used in the RELAP5-3D model. As shown in Figure 5.7 the burnup experienced by the pin changes with axial location so an averaged burnup value of 50.867 (GWd/MTU) was supplied to the thermal conductivity correlation.

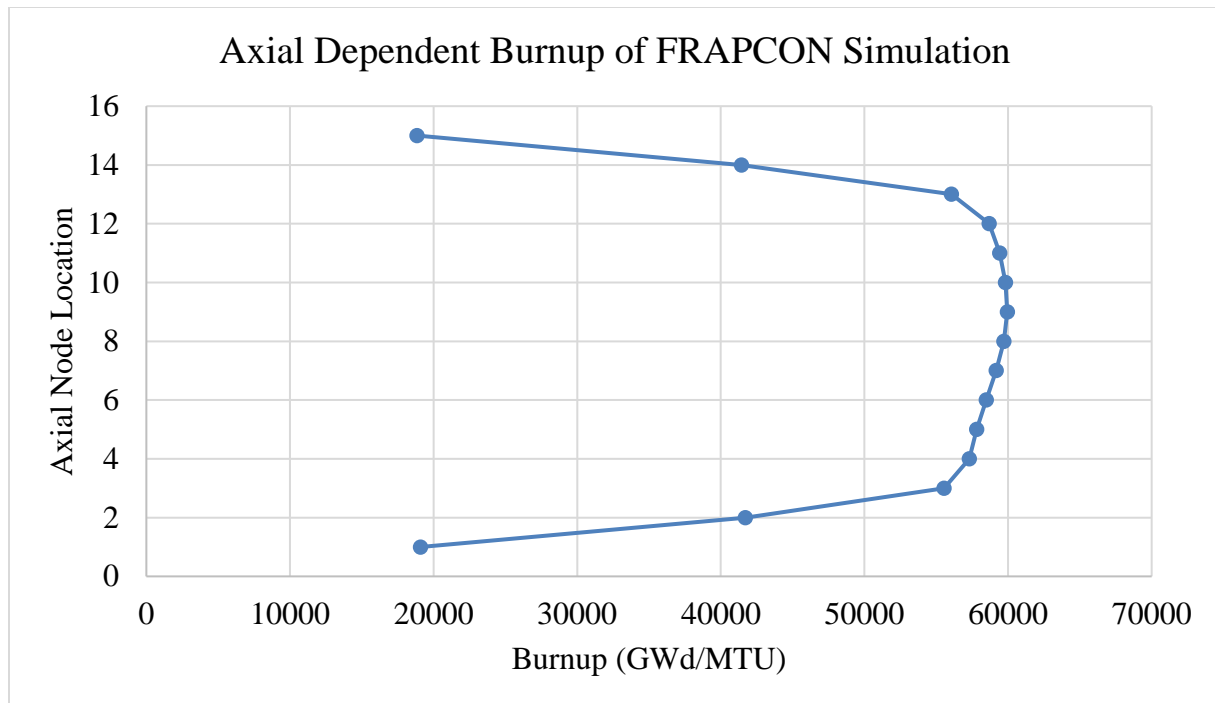


Figure 5.7: Axial Dependent Burnup at Last Time-Step of FRAPCON-4.0 Simulation.

Table 5.3 below gives the temperature-dependent fuel thermal conductivities that are supplied to the RELAP5-3D model.

Table 5.3: Fuel Thermal Conductivity table used in RELAP5-3D model.

Temperature (°F)	Thermal Conductivity (Btu/s·ft·°F)
80.33	0.000509
260.33	0.000472
440.33	0.00044
620.33	0.000413
800.33	0.000391
980.33	0.000376
1160.33	0.000365
1340.33	0.000357
1520.33	0.00035
1700.33	0.00034
1880.33	0.00033
2060.33	0.000319
2240.33	0.000309
2420.33	0.000301
2600.33	0.000294
2780.33	0.00029
2960.33	0.000289

5.3.2 Gap Conductance Models

When analyzing the simulation results between the fuel performance model and the system code model it is important to understand how each model calculates the gap conductance. The conduction across the gap is calculated by the dynamic gap conductance model in the RELAP5-3D model which use a slightly different approach then the FRAPCON-4.0 code. This section provides a detailed description of each codes gap conduction model.

The RELAP5-3D user manual indicates that the dynamic gap conductance model defines an effective gap conductivity based on a simplified deformation model [6]. The gap conductance through the gas is inversely proportional to the size of the gap. Since the longitudinal axis of the fuel pellets is usually offset from the one of the cladding, the width of the fuel-cladding gap varies with azimuthal position as shown in Figure 5.8, which was provided by the theory manual

[6]. The variation in width causes the conductance through the gas in the fuel-cladding gap to vary with azimuthal position. The gap conductance considers this variation by dividing the gap into several segments of equal length, as shown in Figure 5.8.

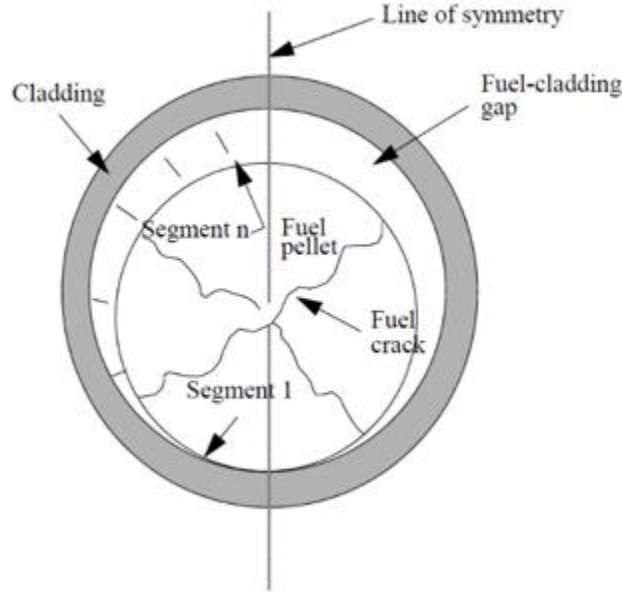


Figure 5.8: Segmentation of the gap in the RELAP5-3D dynamic gap conductance model.

The conductance across the entire gap is calculated as the average conductance of the gas in the segments and is denoted by h_{gas} in Equation 5.3.4.

$$h_{\text{gas}} = \frac{k_g}{N} \sum_{n=1}^N \frac{1}{t_n + 3.2(R_F + R_C) + (g_1 + g_2)} \quad (5.3.4)$$

The azimuthal segmentation approach adopted in RELAP5-3D to calculate the gap conductance is different from the approach adopted by FRAPCON-4.0. The approach used by the fuel performance code to calculate the gap conductance is the summation of the three terms shown in Equation 5.3.5 [15].

$$h_{\text{gap}} = h_{\text{gas}} + h_r + h_{\text{solid}} \quad (5.3.5)$$

The h_r term in Equation 5.3.5 accounts for radiation effects in the gap, h_{gas} provides the gas conductance, and h_{solid} is the increase conductance due to solid-to-solid contact between the surfaces and h_r is the conductance due to radiant heat transfer. To help describe the differences between the two code's gap conduction models Table 5.4 provides a comparison of the FRAPCON-4.0 gas conduction term compared to the gas conduction calculated by the RELAP5-3D dynamic gap conductance model.

Table 5.4: FRAPCON-4.0 and Relap5-3D Gap Conductance Model Breakdown of Gas
Conductance [6] [15]

FRAPCON-4.0 Gap Conductance	Relap5-3D Gap Conductance																																																
$h_{\text{gap}} = h_{\text{gas}} + h_r + h_{\text{solid}}$	$h_{\text{gas}} = \frac{k_{\text{gas}}}{N} \sum_{n=1}^N \frac{1}{t_n + 3.2(R_f + R_c) + (g_f + g_c)}$																																																
FRAPCON-4.0 Gas Conductance	Relap5-3D Gas Conductance																																																
$h_{\text{gas}} = \frac{k_{\text{gas}}}{\Delta x}$	$h_{\text{gas}} = \text{conductance through the gas in the gap (W/m}^2\text{•K)}$																																																
k_{gas} = gas thermal conductivity (W/m•K)	k_{gas} = thermal conductivity of gas (W/m•K)																																																
$K_{\text{gas}} = AT_{\text{gas}}^B$ T_g = gas temperature (K) The constants A and B are fitting parameters used in gas thermal conductivity correlations <table><tr><td>Gas</td><td>A</td><td>B</td></tr><tr><td>He</td><td>2.531x10-3</td><td>0.7146</td></tr><tr><td>Ar</td><td>4.092x10-4</td><td>0.6748</td></tr><tr><td>Kr</td><td>1.966x10-4</td><td>0.7006</td></tr><tr><td>Xe</td><td>9.825x10-5</td><td>0.7334</td></tr><tr><td>H2</td><td>1.349x10-3</td><td>0.8408</td></tr><tr><td>N2</td><td>2.984x10-4</td><td>0.7799</td></tr><tr><td>Air</td><td>1.945x10-4</td><td>0.8586</td></tr></table>	Gas	A	B	He	2.531x10-3	0.7146	Ar	4.092x10-4	0.6748	Kr	1.966x10-4	0.7006	Xe	9.825x10-5	0.7334	H2	1.349x10-3	0.8408	N2	2.984x10-4	0.7799	Air	1.945x10-4	0.8586	$K_{\text{gas}} = AT_{\text{gas}}^B$ T_g = gas temperature (K) The constants A and B are fitting parameters used in gas thermal conductivity correlations <table><tr><td>Gas</td><td>A</td><td>B</td></tr><tr><td>He</td><td>2.639x10-3</td><td>0.7085</td></tr><tr><td>Ar</td><td>2.986x10-4</td><td>0.7224</td></tr><tr><td>Kr</td><td>8.247x10-4</td><td>0.8363</td></tr><tr><td>Xe</td><td>4.351x10-5</td><td>0.8616</td></tr><tr><td>H2</td><td>1.097x10-3</td><td>0.8785</td></tr><tr><td>N2</td><td>5.314x10-4</td><td>0.6898</td></tr><tr><td>Air</td><td>1.853x10-4</td><td>0.8729</td></tr></table>	Gas	A	B	He	2.639x10-3	0.7085	Ar	2.986x10-4	0.7224	Kr	8.247x10-4	0.8363	Xe	4.351x10-5	0.8616	H2	1.097x10-3	0.8785	N2	5.314x10-4	0.6898	Air	1.853x10-4	0.8729
Gas	A	B																																															
He	2.531x10-3	0.7146																																															
Ar	4.092x10-4	0.6748																																															
Kr	1.966x10-4	0.7006																																															
Xe	9.825x10-5	0.7334																																															
H2	1.349x10-3	0.8408																																															
N2	2.984x10-4	0.7799																																															
Air	1.945x10-4	0.8586																																															
Gas	A	B																																															
He	2.639x10-3	0.7085																																															
Ar	2.986x10-4	0.7224																																															
Kr	8.247x10-4	0.8363																																															
Xe	4.351x10-5	0.8616																																															
H2	1.097x10-3	0.8785																																															
N2	5.314x10-4	0.6898																																															
Air	1.853x10-4	0.8729																																															
Δx = total effective gap width (m) $\Delta x = d_{\text{eff}} + 1.8 (g_f + g_c) - b + d$ $d_{\text{eff}} = \exp (-0.00125P) R_f + R_c,$ for closed fuel-cladding gaps (m) d_{eff} = $R_f + R_c$ for open fuel-cladding gaps (m) $b = 1.397 \times 10^{-6}$ (m) d = value from FRACAS for open fuel-cladding gap size (m)	t_n = width of fuel-cladding gap at the midpoint of the n-th circumferential segment (m) $t_n = \left(\frac{2 n - 1}{N} \right) t_g$ and $t_g = t_o - u_F + u_C$ n = number of circumferential segment N = total number of circumferential segments = 8 u_F = radial displacement of the fuel pellet surface (m) u_C = radial displacement of cladding inner surface (m).																																																
$R_f + R_c$ = cladding plus fuel surface roughness (m)	$R_f + R_c$ = cladding plus fuel surface roughness (m)																																																
$(g_f + g_c)$ = temperature jump distances at fuel and cladding surfaces, respectively (m)	$(g_f + g_c)$ = temperature jump distances at fuel and cladding surfaces, respectively (m)																																																

Table 5.4 shows that a few difference between each code's gas conduction models exist. The first difference occurs in each code's correlation for determining the gas thermal conductivity. The second difference occurs in each code's method of calculating the gap size, which is the total effective gap in the FRAPCON-4.0 model and the width of the averaged fuel-cladding gap of the circumferential segments in the RELAP5-3D model. The FRAPCON-4.0 total effective gap relies on a values obtained from the codes mechanical model FRACAS. The FRACAS model calculates the small displacement deformation of the fuel and cladding based of analysis including the effects of fuel thermal expansion, swelling, densification, and relocation; cladding thermal expansion, creep, and plasticity; fission gas and external coolant pressures [15]. The RELAP5-3D gap conduction model considers material mechanics in the gap width term t_n which is a function of the radial displacement of the fuel pellet surface and cladding inner surface. The radial displacement of the fuel pellet surface is based of analysis of the fuel thermal expansion, swelling, densification, and relocation while the displacement of the cladding inner surface is based of analysis of cladding thermal expansion, creep, and plasticity. Although both codes approach the conductivity of the gap in different was their methods of calculating the conduction of the gas share many similarities. The FRAPCON-4.0 code also considers the conduction of the gap due to solid-to-solid contact and radiation described by Equation 5.3.6 and Equation 5.3.7 respectively.

$$h_r = \sigma F (T_{fs}^2 + T_{ci}^2) (T_{fs} + T_{ci})$$

$$F = \frac{1}{e_f + \left(\frac{r_{fs}}{r_{ci}}\right) \left(\frac{1}{e_c} - 1\right)} \quad (5.3.6)$$

Where,

σ = Stefan-Boltzman constant = 5.6697E-8 (W/m²-K⁴)

e_f = fuel emissivity

e_c = cladding emissivity

T_{fs} = fuel surface temperature (K)

T_{ci} = cladding inner surface temperature (K)

r_{fs} = fuel outer surface radius (m)

r_{ci} = cladding inner surface radius (m)

$$h_{solid} = \frac{0.4166K_m P_{rel} R_{mult}}{R * E} P_{rel} > 0.003$$

$$h_{solid} = \frac{0.00125K_m}{R * E} 0.003 > P_{rel} > 9 \times 10^{-6} \quad (5.3.7)$$

$$h_{solid} = \frac{0.4166K_m P_{rel}^{0.5}}{R * E} P_{rel} < 9 \times 10^{-6}$$

Where,

P_{rel} = ratio of interfacial pressure to cladding Meyer hardness (approximately 680 MPa)

K_m = geometric mean conductivity (W/m-K) = $2k_f k_c / (k_f + k_c)$

$R = \sqrt{R_f^2 + R_c^2}$ (m), where R_f and R_c are the roughness of the fuel and cladding (m)

$R_{mult} = 333.3 P_{rel}$, if $P_{rel} \leq 0.0087$

$R_{mult} = 2.9$, if $P_{rel} > 0.0087$

k_c = cladding thermal conductivity (W/m-K)

k_f = fuel thermal conductivity (W/m-K)

$E = \exp[5.738 - 0.528 \ln(3.937 \times 10^7 R_f)]$

6 FRAPCON-4.0 AND RELAP5-3D SIMULATION RESULTS

The simulation results helped determine the path of developing a couple between the system code RELAP5-3D and fuel performance code FRAPCON-4.0. Parameters of the final model, described in the previous section, were adopted after preliminary results lead to model refinement. This section includes a brief discussion of the preliminary model simulations which motivated improvements to the system code model used in final code comparison analysis.

6.1 Preliminary RELAP5-3D Model Simulation Results

The differences between the initial system code model used, for model refinement, and the final model includes the radial power profile and fuel thermal conductivity table supplied to the model. The initial system code model was supplied the radial power profile from the fuel performance model of an axial node located at the center of the fuel pin. It was also supplied the stored fuel thermal properties of the RELAP5-3D system code. Results of this initial model are shown in Figure 6.1 which compare the radial temperature profile, at center axial node, of the simulation results of both codes.

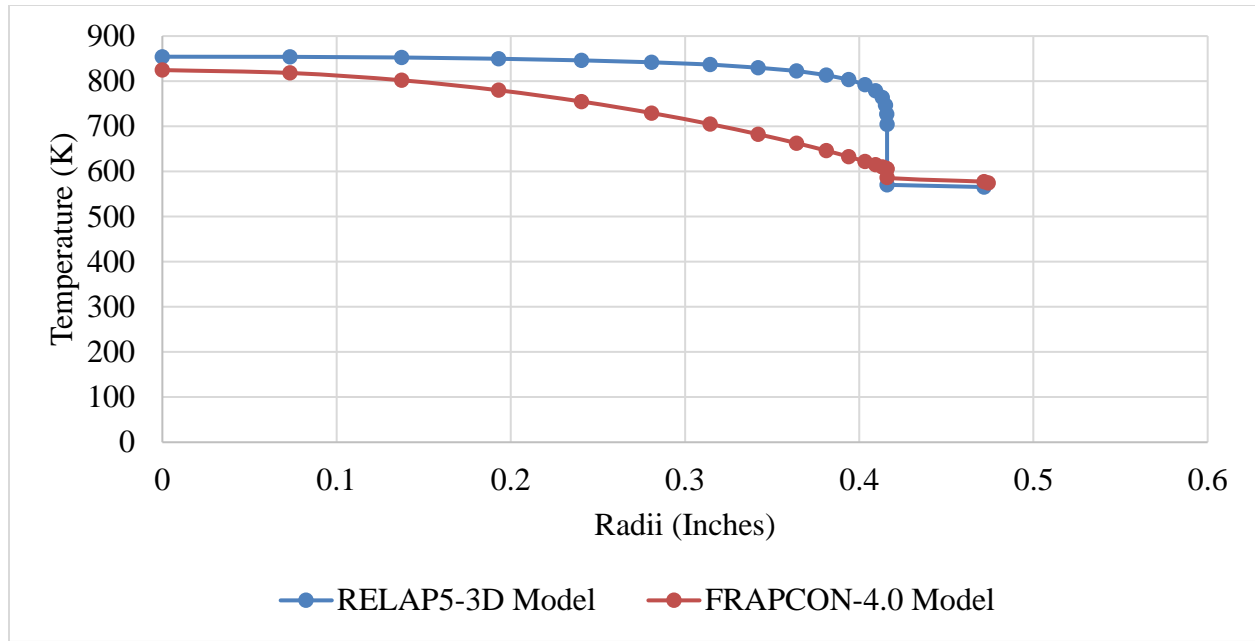


Figure 6.1: Radial temperature profile of the initial model at the center axial node.

The simulation results motivated the detailed analysis of the fuel thermal conductivity model used by the FRAPCON-4.0 code as described by its theory manual. The RELAP5-3D model was improved by supplying the fuel thermal conductivity as a function of temperature related directly to the FRAPCON-4.0 modified NFI model described in the previous section. Simulation results comparing the fuel performance simulation to the improved system code model with the thermal conductivity table generated from the FRAPCON-4.0 theory manual are shown in Figure 6.2.

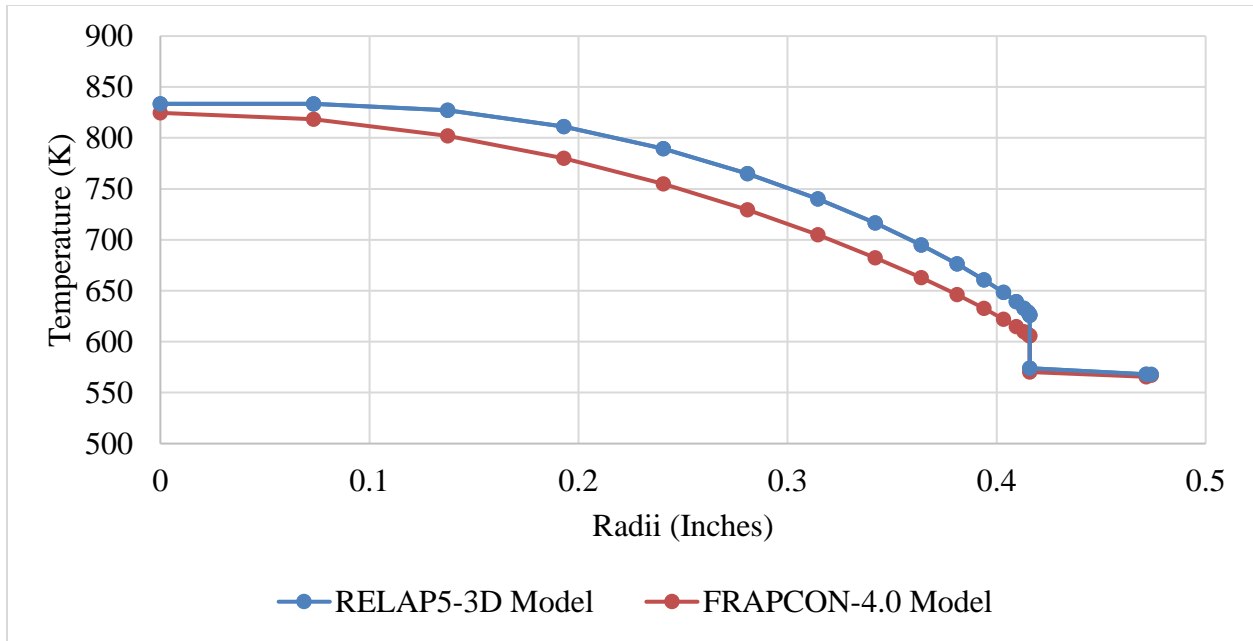


Figure 6.2: Center axial node radial temperature profile simulation results of refined system code model with modified fuel thermal conductivity properties.

Simulation results of the system code model containing the revised fuel thermal conductivity properties yield a radial temperature distribution much closer to the fuel performance simulation results. Figure 6.2 indicates that the use of the center radial power profile imposes a slightly higher radial temperature distribution in the system code simulation than in the fuel performance code simulation. The final RELAP5-3D model was refined to take an averaged radial power profile from the FRAPCON-4.0 model which was supplied to all axial locations. The modified system code model including the averaged radial power profile is compared the to the FRAPCON-4.0 simulation at the center axial node as shown in Figure 6.3.

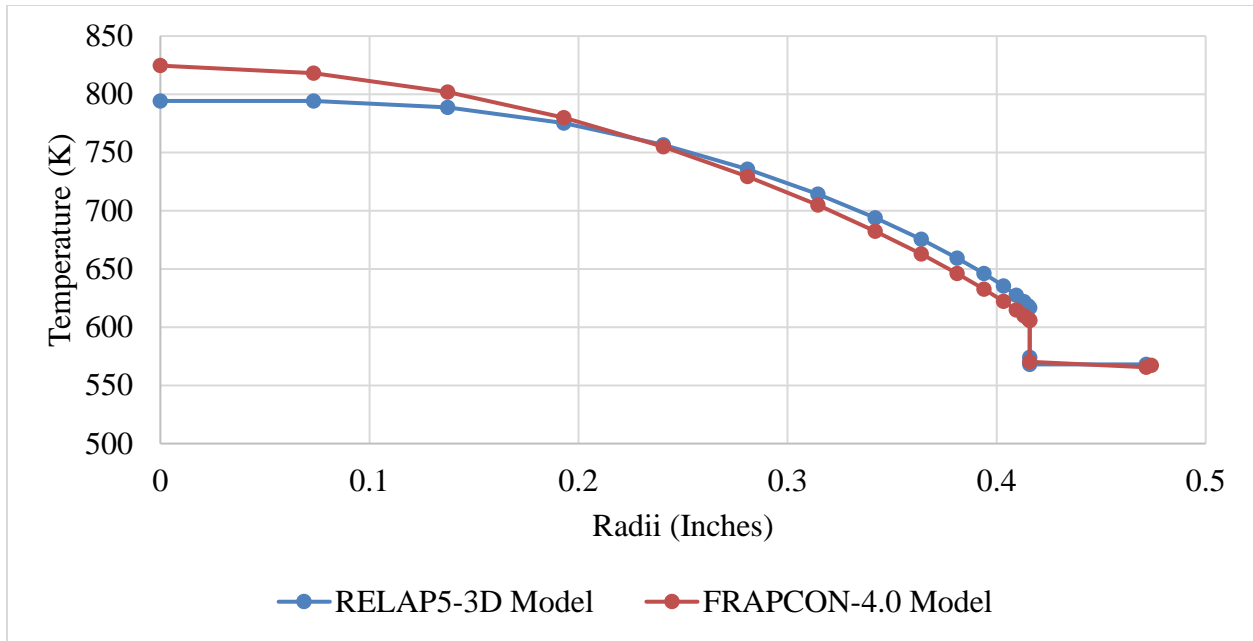


Figure 6.3: Center axial node radial temperature profile simulation results of refined system code model with averaged radial power profile.

Figure 6.3 shows that the averaged power profile approach supplied to the system code model distributes the temperature profile in a similar manner compared to the fuel performance simulation. The radial temperature profiles are not exact matches at this axial location but a stored energy calculation was performed to determine if the physical phenomena between codes is preserved. The results of the stored energy calculation are presented for every axial location in the following section.

6.2 Final RELAP5-3D Model Simulation Results

After the system code model was refined to better match the fuel performance model a simulation was performed and the results were used to make a comparison between the two code models. The following figures provide the radial temperature profiles of the first axial node (a region near the bottom of the fuel pin) Figure 6.4, seventh axial node (a region near the center of

the fuel pin) Figure 6.5, and the fifteen the axial node (a region near the top of the fuel pin)
Figure 6.6.

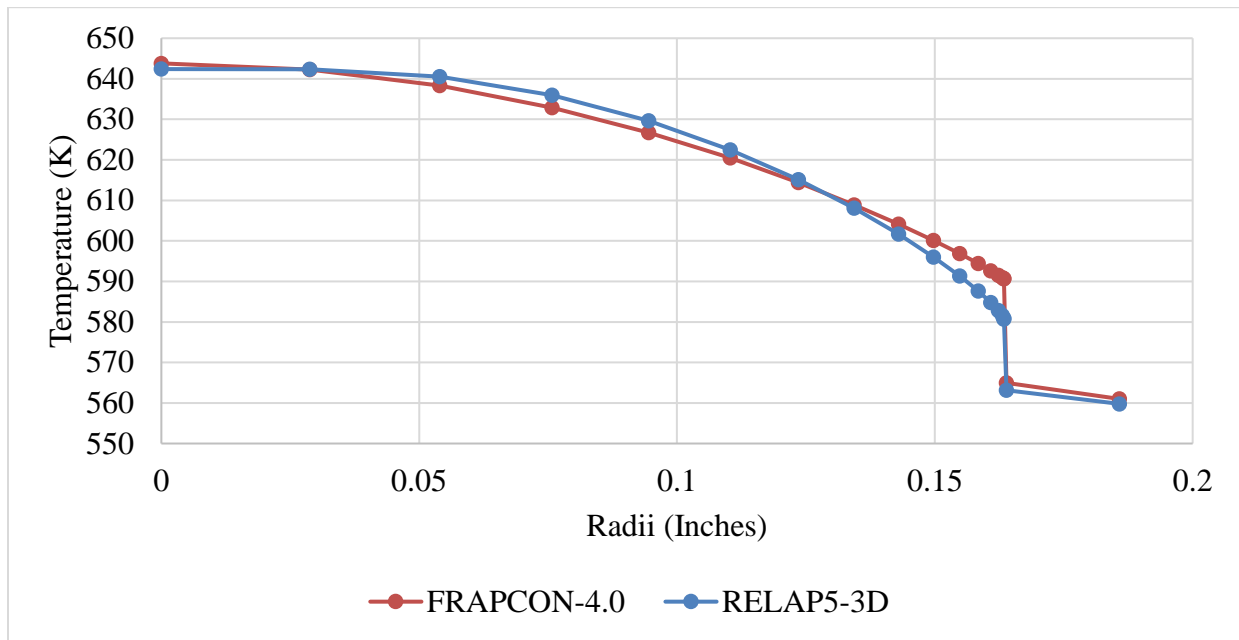


Figure 6.4: FRAPCON-4.0 and RELAP5-3D comparison results of radial temperature profiles at
the first axial node.

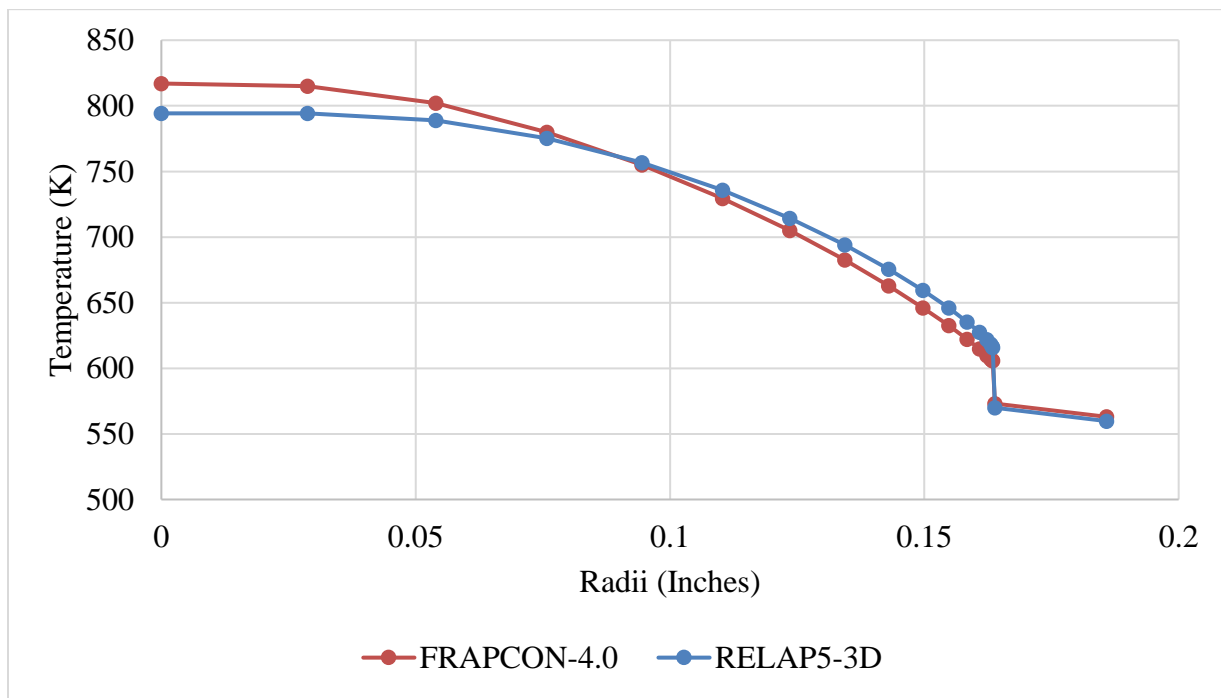


Figure 6.5: FRAPCON-4.0 and RELAP5-3D comparison results of radial temperature profiles at the seventh axial node.

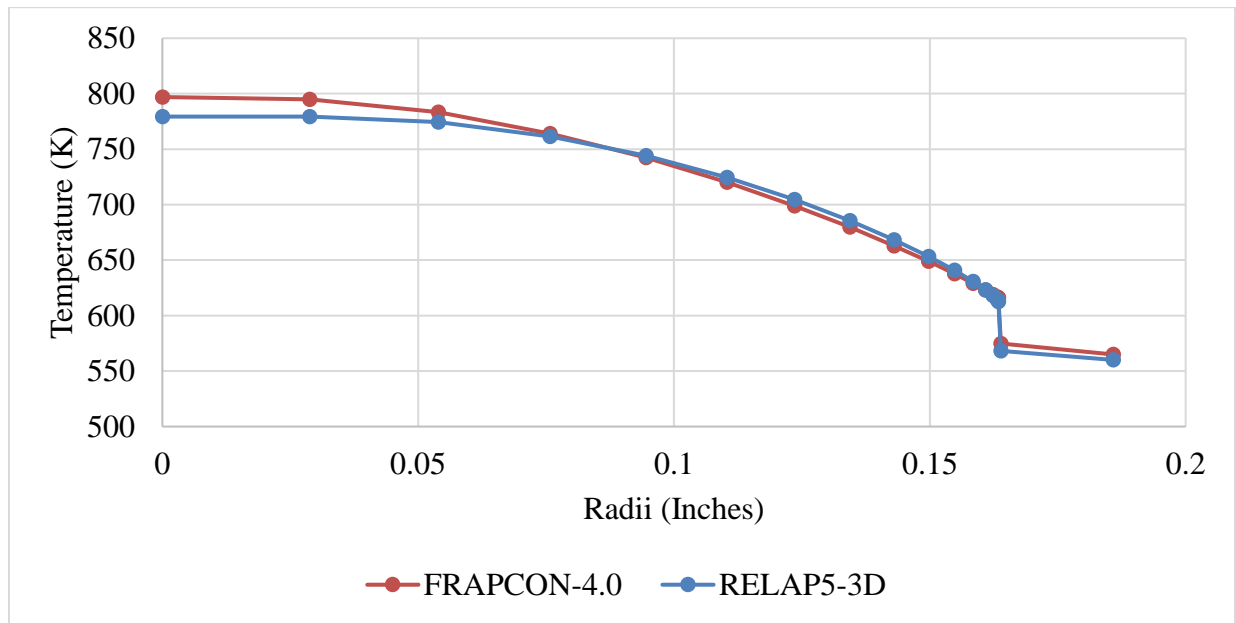


Figure 6.6: FRAPCON-4.0 and RELAP5-3D comparison results of radial temperature profiles at the fifteenth axial node.

As shown in the radial temperature comparison plots of each code the profiles do not match exactly at every axial node due to the averaging method applied to the radial power distribution of the system code model. Even though these temperature profiles are not exact matches the stored energy analysis suggest preservation of physical phenomena. Table 6.1 gives the results of the calculated stored energy of the system code model compared to the stored energy calculated by the FRAPCON-4.0 model for each axial location. The results provided in Table 6.1 show the relative error calculated for all axial locations is less than 10%. Unfortunately, the FRAPCON-4.0 model gives the stored energy result as a crude value rounded to two decimal places which indicates that the relative error could vary if more decimal places are provided by the FRAPCON-4.0 simulation results. To obtain a more accurate comparison

between the codes' calculated stored energies the FRAPCON-4.0 simulation results will need to provide more decimals.

Table 6.1: Stored energy comparison between the RELAP5-3D model and FRAPCON-4.0 model.

Axial Node	Stored Energy (J/kg)		% Error
	FRAPCON-4.0	RELAP5-3D	
1	8.70E+04	8.80E+04	1.14%
2	1.10E+05	1.10E+05	0.00%
3	1.10E+05	1.10E+05	0.00%
4	1.10E+05	1.10E+05	0.00%
5	1.10E+05	1.20E+05	8.33%
6	1.20E+05	1.20E+05	0.00%
7	1.20E+05	1.30E+05	7.69%
8	1.20E+05	1.30E+05	7.69%
9	1.20E+05	1.20E+05	0.00%
10	1.20E+05	1.20E+05	0.00%
11	1.30E+05	1.30E+05	0.00%
12	1.30E+05	1.40E+05	7.14%
13	1.30E+05	1.30E+05	0.00%
14	1.20E+05	1.20E+05	0.00%
15	9.60E+04	9.40E+04	-2.13%

7 BISON AND FRAPCON-4.0 MODEL DEVELOPMENT

7.1 BISON Model Development

A single pin BISON model will serve as the primary reference for the preparation of a FRAPCON-4.0 model. The reference BISON model represents a single fuel rod of a typical PWR. The model is prepared to simulate the behavior of the fuel pin through two fuel cycles. Characteristics of a typical Westinghouse PWR fuel pin were found in publicly available sources. Table 7.1 provides a list of the main parameters used to prepare the model and their respective source.

Table 7.1: General BISON Model Parameters

Parameter	BISON Value	Source Value	Source
Cladding Thickness	0.57 mm	0.573 mm	University of Tennessee [16]
Cladding Bottom Gap	1 mm	1 mm	Massachusetts Institute of Technology [17]
Cladding Top Gap	0.1599 m	0.16 m	Westinghouse [11]
Cladding Roughness	2.00E-06	2.00E-06	Westinghouse [11]
Gas Fill Pressure	20 MPa	20 MPa	Massachusetts Institute of Technology [17]
Fuel/Clad Gap Width	8.4e-05 m	8.4e-05 m	University of Tennessee [16]
Fuel Enrichment	4.8%	4.8%	Massachusetts Institute of Technology [17]
Fuel Density	10.2663 gm/cm ³	94% of Theoretical (10.97 gm/cm ³)	Massachusetts Institute of Technology [17]
Fuel Roughness	1.00E-06	1.00E-06	Westinghouse [11]
Pellet Inner Radius	0 m	0 m	University of Tennessee [16]
Pellet Outer Radius	4.095 mm	Fuel Dia. = (8.19 mm / 2) = 4.095 mm	Massachusetts Institute of Technology [17]
Pellet Quantity	372	372	Massachusetts Institute of Technology [17]
Pellet Height	9.83 mm	9.8 mm	Massachusetts Institute of Technology [17]
Active Fuel Length	3.66 m	3.66 m	Massachusetts Institute of Technology [17]
Rod Pitch	12.6 mm	12.6mm	Massachusetts Institute of Technology [17]
System Pressure	Average value of 15.63 MPa	15.51 MPa	Massachusetts Institute of Technology [17]

The fuel rod of a typical PWR consist of approximately 372 small uranium oxide fuel pellets stacked axially inside a Zircaloy tube cladding. Figure 7.1 shows a diagram of a typical PWR fuel rod [18].

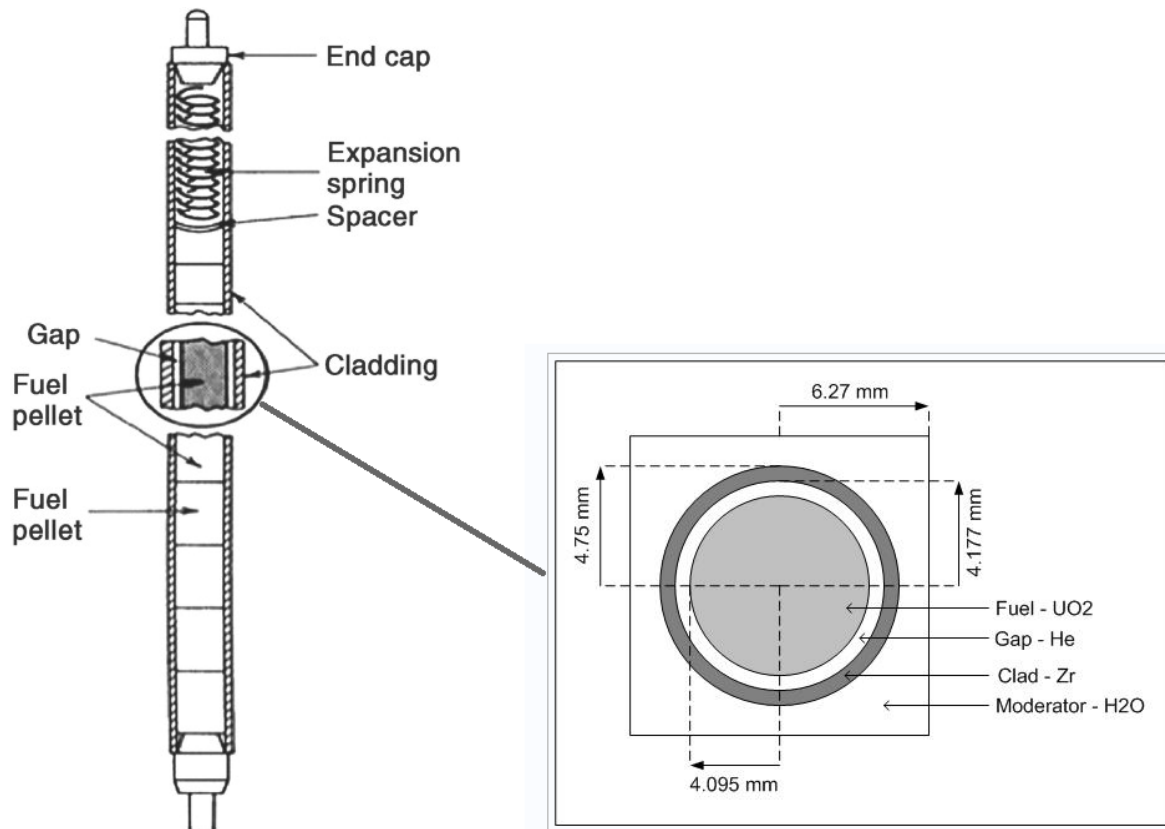


Figure 7.1: Fuel Rod Physical Model Diagram [18]

The BISON single pin model was discretized into 49 axial nodes and 80 radial nodes. The number of axial nodes was chosen to easily model different time-dependent parameters across the length of the pin. The BISON model includes all the time-dependent boundary conditions listed below:

- axial power profile
- inlet coolant temperature
- inlet coolant pressure
- rod average linear heat generation rate
- fast neutron flux

These parameters are supplied to the model in 50-day increments, for a total simulation time of 54 months. This results in 33 time steps data points, simulating three 18-month fuel cycles. The time-dependent parameters supplied to the BISON model are shown below (Figure 7.2- Figure 7.6). The 18-month fuel cycles are included in these figures.

Figure 7.2, provides snapshots of the power profiles at three selected time-steps (initial, middle, and final time-steps) of the simulation. These power profiles were generated by INL's PHISICS; (Parallel and Highly Innovative Simulation for the INL Code System) model of a twice burnt fuel rod.

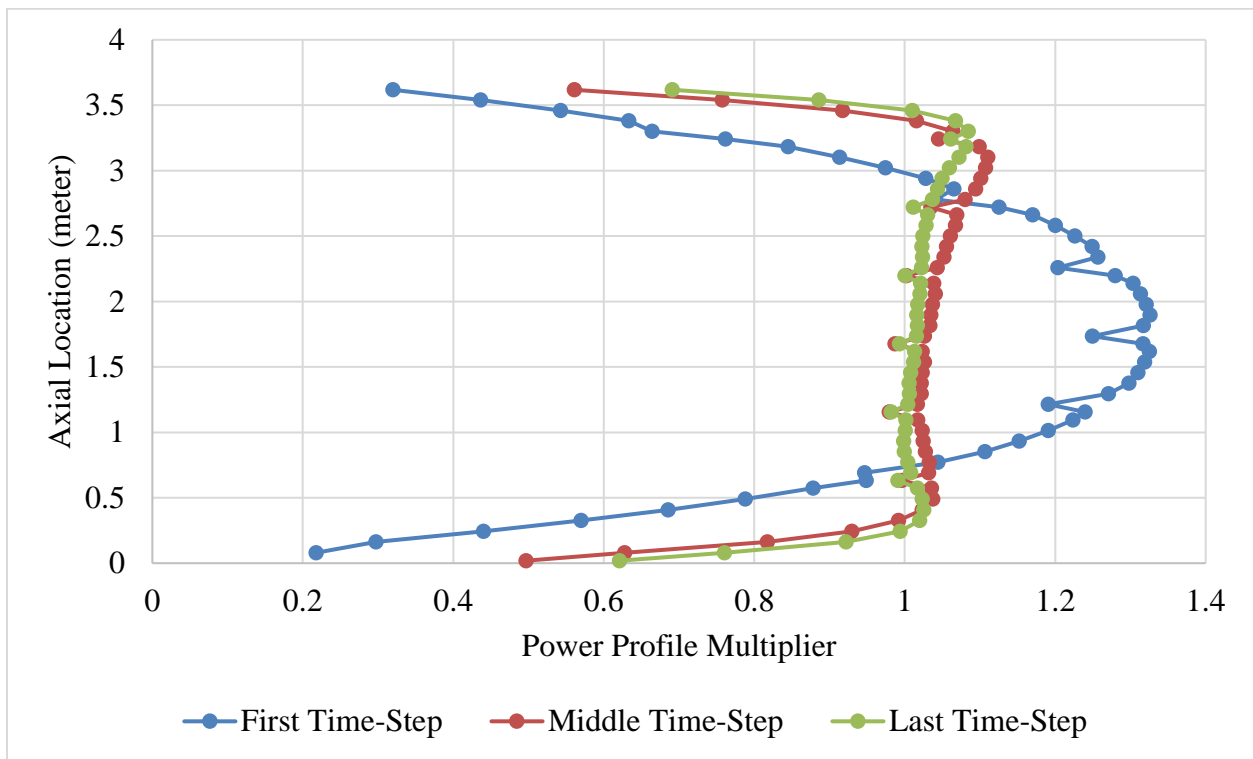


Figure 7.2: Time Dependent Axial Power Profiles

As shown in Figure 7.2, the initial power profile implemented into the BISON model represents a chopped cosine shape, typical of the beginning of the fuel life. As the fuel is spent in the reactor core, the power profile skews toward the top, assuming the typical double peak shape.

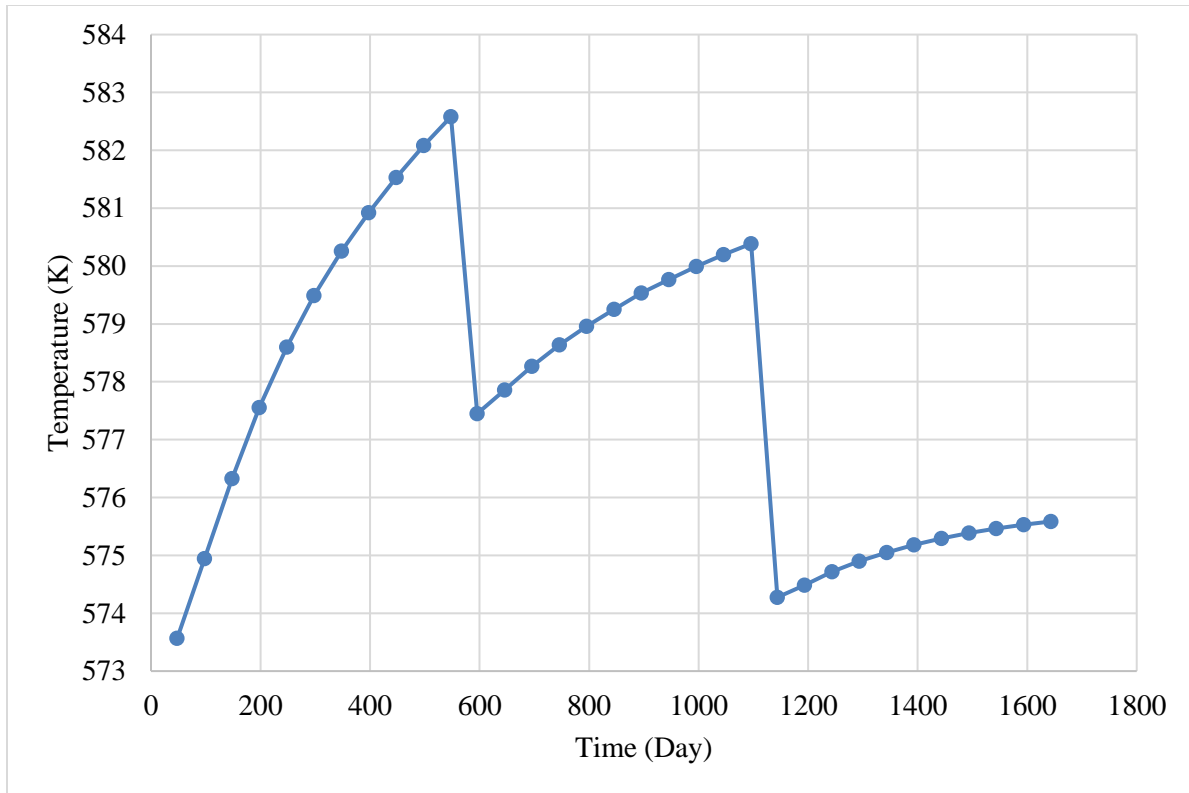


Figure 7.3: Time-Dependent Coolant Inlet Temperature

In Figure 7.3, the average inlet temperature is 572 K and the initial coolant inlet temperature (first time step) is approximately 583 K.

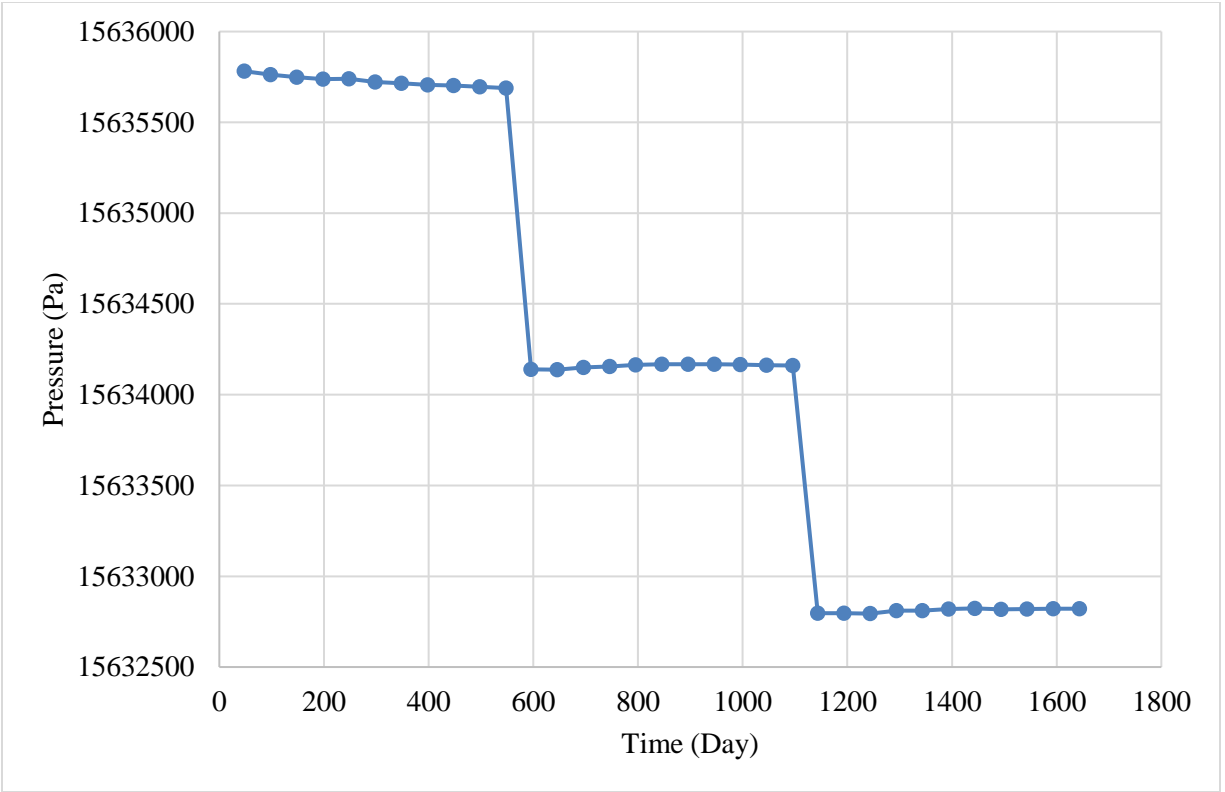


Figure 7.4: Time-Dependent Coolant Inlet Pressure

The coolant inlet pressure in the Figure 7.4 has an averaged value of 15.63 MPa which is slightly higher than the typical PWR pressure of 15.51MPa given in . It was decided to match the slightly higher coolant inlet temperature of the coolant defined in the model to preserve the same subcooling level.

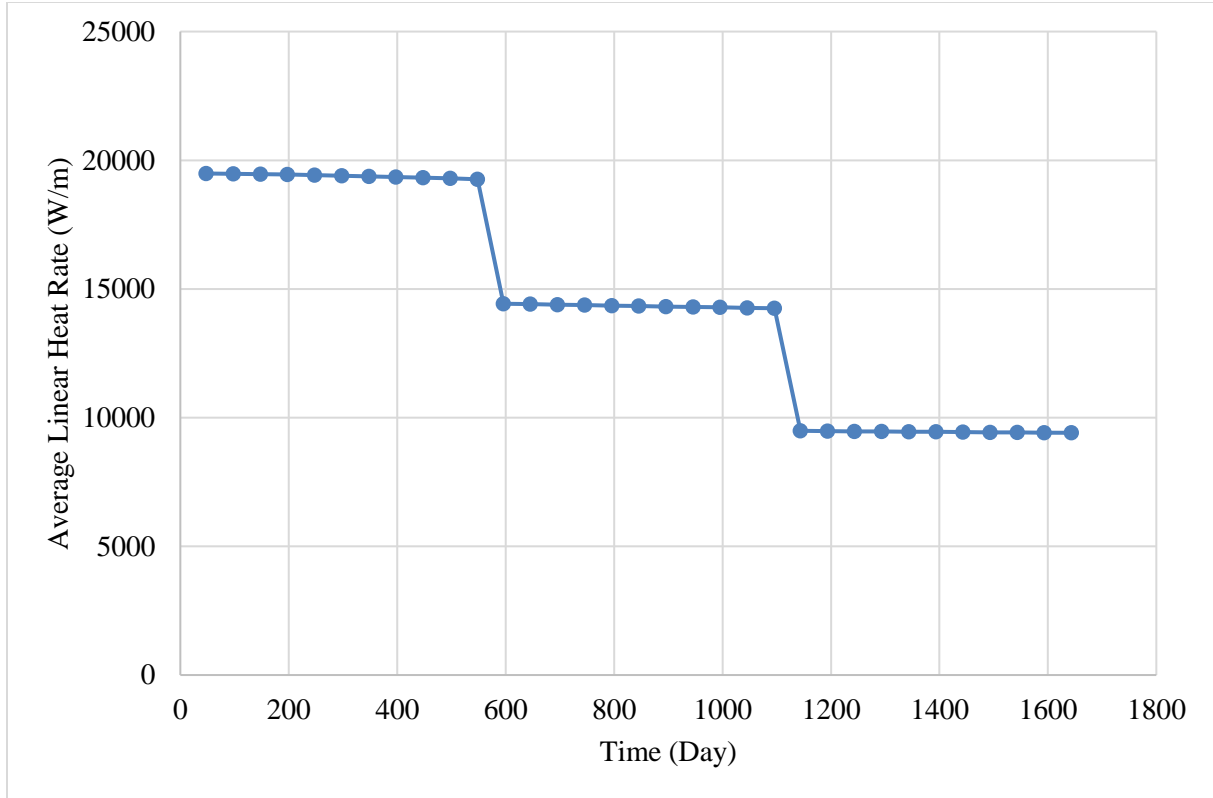


Figure 7.5: Time-Dependent Average Linear Heat Generation Rate

The average linear heat generation rate is about 19,000 W/m for the first 18-month cycle, 14,000 W/m for the second, and 9,000W/m for the third. This corresponds to an average heat flux of approximately 738,000 W/m², 544,000 W/m², and 350,000 W/m² respectively. These values agree with the average heat flux of a typical PWR specified in as 598,000 W/m².

The time-dependent fast flux provided by Figure 7.6 supplies the BISON model with an averaged fast flux of $6.60\text{E}+16 \frac{n}{m^2s}$ over the first 18-moth fuel cycle. For the second and third fuel cycles the average fast flux supplied to the BISON model are $5.75\text{E}+17 \frac{n}{m^2s}$ and $4.19\text{E}+17 \frac{n}{m^2s}$ respectively.

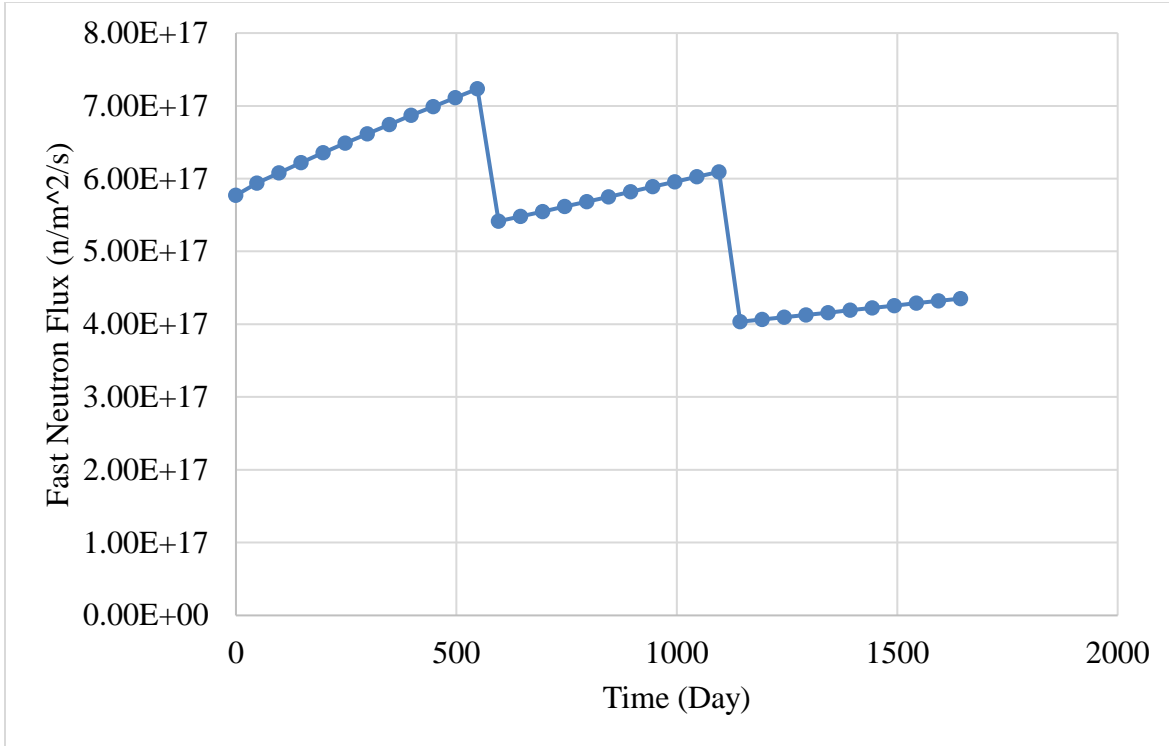


Figure 7.6: Time-dependent fast neutron flux

7.2 FRAPCON-4.0 Model Development

The BISON fuel performance code, currently under development, will replace the FRAPCON-4.0 code in future applications. Thanks to the similarities between the codes, the parameters used to build the FRAPCON-4.0 fuel pin model are very similar to the ones previously described. All the general parameters defined in the BISON model were directly applied to the FRAPCON-4.0 model input deck and are given in Table 7.2.

Table 7.2: FRAPCON-4.0 general parameters used to build a single pin model.

Parameter used in both of the BISON and FRAPCON-4.0 models	Value
Cladding Thickness	0.57 mm
Cladding Bottom Gap	1 mm
Cladding Top Gap	0.1599 m
Cladding Roughness	2.00E-06
Gas Fill Pressure	2.0 Mpa
Fuel/Clad Gap Width	0.084 mm
Fuel Enrichment	4.80%
Fuel Density	10.2663 kg/m ³
Fuel Roughness	1.00E-06
Pellet Inner Radius	0 m
Pellet Outer Radius	4.095 mm
Pellet Height	9.83 mm
Active Fuel Length	3.66 m
Rod Pitch	12.6 mm

To simplify the comparison between the two fuel performance code simulations the axial discretization of the geometry was aligned. The FRAPCON-4.0 pin model was subdivided into 49 axial nodes which is adopted from the BISON model to allow the implementation of different time-dependent axial parameters. Each of the 49 axial nodes was discretized into 40 radial segments by the FRAPCON-4.0 code, which is half the resolution of the BISON model. The radial boundaries of the fuel pellet segments are automatically spaced by the code with greater fraction in the outer region to optimize the heat generation radial distribution through the pin.

The FRAPCON-4.0 model was supplied the BISON time-dependent boundary conditions which include:

- inlet coolant temperature
- inlet coolant pressure

- rod average linear heat generation rate
- fast neutron flux
- radial power distributions

These parameters are supplied to the model in the same 50-day increments used by the BISON model. The FRAPCON-4.0 model's total simulation time of 54 months which is divided into 33 time steps data points. The time-depend parameters supplied to the FRAPCON-4.0 model can be seen above (Figure 7.2-Figure 7.6). The three 18-month fuel cycles are included in these figures.

7.3 Material Properties Description

7.3.1 Fuel Thermal Conductivity

The fuel performance code BISON has five empirical models available to calculate the UO₂ thermal conductivity. These correlations consist of the Fink-Lucuta [19] [20], Halden [9], NFIR [21], MATPRO [13], and modified NFI models [22] [14]. Each correlation model was developed through the evolution process which lead to a more accurate prediction of thermal conductivity of the fuel. For example, the MATPRO model was followed by the Fink-Lucuta model which accounted for burnup degradation. Then the Fink-Lucuta model was surpassed by the NFI model since the model suffered from a weak degradation term. The NFI model was eventually modified by PNNL to better fit UO₂ experimental data and it also allowed MOX fuel thermal conductivities to be computed [22]. The modified NFI model is used to calculate fuel thermal conductivity in FRAPCON-4.0 because it is the most evolved correlation. Since this model is used by FRAPCON-4.0 and is adopted by the BISON model simplifies comparison

analysis between the fuel performance codes. (Refer to the material property section of the FRAPCON-40 and RELAP5-3D model development section of this report for the detail description of the modified NFI model.)

7.3.2 Gap Conductance

The approach used by both fuel performance codes to calculate the gap conductance is the summation of the three terms shown in Equation [15].

$$h_{\text{gap}} = h_{\text{gas}} + h_r + h_{\text{solid}} \quad (.8)$$

The h_r term in Equation accounts for radiation effects in the gap, h_{gas} provides the gas conductance, and h_{solid} is the increase conductance due to solid-to-solid contact between the surfaces and h_r is the conductance due to radiant heat transfer. To help describe the differences between the two code's gap conductance models Table 7.3 provides a comparison between them.

Table 7.3: FRAPCON-4.0 and BISON Gap Conductance Model Comparison [22] [12]

FRAPCON-4.0 Gap Conductance	BISON Gap Conductance																																																
$h_{\text{gap}} = h_{\text{gas}} + h_{\text{r}} + h_{\text{solid}}$	$h_{\text{gap}} = h_{\text{gas}} + h_{\text{r}} + h_{\text{solid}}$																																																
FRAPCON-4.0 Gas Conductance	BISON Gas Conductance																																																
$h_{\text{gas}} = \frac{k_{\text{gas}}}{\Delta x}$	$h_{\text{gas}} = \frac{k_{\text{gas}}}{d_{\text{g}} + C_{\text{r}} (R_{\text{f}} + R_{\text{c}}) + g_{\text{f}} + g_{\text{c}}}$																																																
k_{gas} = gas thermal conductivity (W/m-K)	k_{gas} = thermal conductivity of gas (W/m•K)																																																
$K_{\text{gas}} = AT_{\text{gas}}^B$ T_{g} = gas temperature (K) The constants A and B are fitting parameters used in gas thermal conductivity correlations	$K_{\text{gas}} = AT_{\text{gas}}^B$ T_{g} = gas temperature (K) The constants A and B are fitting parameters used in gas thermal conductivity correlations																																																
<table><tr><td>Gas</td><td>A</td><td>B</td></tr><tr><td>He</td><td>2.531x10-3</td><td>0.7146</td></tr><tr><td>Ar</td><td>4.092x10-4</td><td>0.6748</td></tr><tr><td>Kr</td><td>1.966x10-4</td><td>0.7006</td></tr><tr><td>Xe</td><td>9.825x10-5</td><td>0.7334</td></tr><tr><td>H2</td><td>1.349x10-3</td><td>0.8408</td></tr><tr><td>N2</td><td>2.984x10-4</td><td>0.7799</td></tr><tr><td>Air</td><td>1.945x10-4</td><td>0.8586</td></tr></table>	Gas	A	B	He	2.531x10-3	0.7146	Ar	4.092x10-4	0.6748	Kr	1.966x10-4	0.7006	Xe	9.825x10-5	0.7334	H2	1.349x10-3	0.8408	N2	2.984x10-4	0.7799	Air	1.945x10-4	0.8586	<table><tr><td>Gas</td><td>A</td><td>B</td></tr><tr><td>He</td><td>2.639x10-3</td><td>0.7085</td></tr><tr><td>Ar</td><td>2.986x10-4</td><td>0.7224</td></tr><tr><td>Kr</td><td>8.247x10-4</td><td>0.8363</td></tr><tr><td>Xe</td><td>4.351x10-5</td><td>0.8616</td></tr><tr><td>H2</td><td>1.097x10-3</td><td>0.8785</td></tr><tr><td>N2</td><td>5.314x10-4</td><td>0.6898</td></tr><tr><td>Air</td><td>1.853x10-4</td><td>0.8729</td></tr></table>	Gas	A	B	He	2.639x10-3	0.7085	Ar	2.986x10-4	0.7224	Kr	8.247x10-4	0.8363	Xe	4.351x10-5	0.8616	H2	1.097x10-3	0.8785	N2	5.314x10-4	0.6898	Air	1.853x10-4	0.8729
Gas	A	B																																															
He	2.531x10-3	0.7146																																															
Ar	4.092x10-4	0.6748																																															
Kr	1.966x10-4	0.7006																																															
Xe	9.825x10-5	0.7334																																															
H2	1.349x10-3	0.8408																																															
N2	2.984x10-4	0.7799																																															
Air	1.945x10-4	0.8586																																															
Gas	A	B																																															
He	2.639x10-3	0.7085																																															
Ar	2.986x10-4	0.7224																																															
Kr	8.247x10-4	0.8363																																															
Xe	4.351x10-5	0.8616																																															
H2	1.097x10-3	0.8785																																															
N2	5.314x10-4	0.6898																																															
Air	1.853x10-4	0.8729																																															

Δx = total effective gap width (m) $\Delta x = d_{\text{eff}} + 1.8 (g_f + g_c) - b + d$ $d_{\text{eff}} = \exp (-0.00125P) R_f + R_c$, for closed fuel-cladding gaps (m) $d_{\text{eff}} = R_f + R_c$ for open fuel-cladding gaps (m) $b = 1.397 \times 10^{-6}$ (m) d = value from FRACAS for open fuel-cladding gap size (m)	$d_g + C_r (R_f + R_c) + g_f + g_c$ $d_g = r * \ln \left(\frac{R_f}{R_c} \right)$ C_r = roughness coefficient typically 1.8 for PWRs
$R_f + R_c$ = cladding plus fuel surface roughness (m)	$R_f + R_c$ = cladding plus fuel surface roughness (m)
$(g_f + g_c)$ = temperature jump distances at fuel and cladding surfaces, respectively (m)	$(g_f + g_c)$ = temperature jump distances at fuel and cladding surfaces, respectively (m)
FRAPCON-4.0 Conductance due to radiant heat transfer.	BISON Conductance due to radiant heat transfer
$h_r = \frac{\sigma F (T_{fs}^2 + T_{ci}^2) (T_{fs} + T_{ci})}{1}$ $F = \frac{1}{e_f + \left(\frac{r_{fs}}{r_{ci}} \right) \left(\frac{1}{e_c} - 1 \right)}$	$h_r = \frac{\sigma F (T_{fs}^2 + T_{ci}^2) (T_{fs} + T_{ci})}{1}$ $F = \frac{1}{e_f + \left(\frac{r_{fs}}{r_{ci}} \right) \left(\frac{1}{e_c} - 1 \right)}$
σ = Stefan-Boltzman constant = 5.6697E-8 (W/m ² -K ⁴) e_f = fuel emissivity e_c = cladding emissivity T_{fs} = fuel surface temperature (K) T_{ci} = cladding inner surface temperature (K) r_{fs} = fuel outer surface radius (m) r_{ci} = cladding inner surface radius (m)	σ = Stefan-Boltzman constant = 5.6697E-8 (W/m ² -K ⁴) e_f = fuel emissivity e_c = cladding emissivity T_{fs} = fuel surface temperature (K) T_{ci} = cladding inner surface temperature (K) r_{fs} = fuel outer surface radius (m) r_{ci} = cladding inner surface radius (m)
FRAPCON-4.0 Conductance increase due to solid-to-solid contact.	BISON Conductance increase due to solid-to-solid contact.
$h_{\text{solid}} = \frac{0.4166 K_m P_{\text{rel}} R_{\text{mult}}}{R * E} P_{\text{rel}} > 0.003$ $h_{\text{solid}} = \frac{0.00125 K_m}{R * E} 0.003 > P_{\text{rel}}$ $h_{\text{solid}} = \frac{0.00125 K_m}{R * E} 0.003 > 9 \times 10^{-6}$ $h_{\text{solid}} = \frac{0.4166 K_m P_{\text{rel}}^{0.5}}{R * E} P_{\text{rel}} < 9 \times 10^{-6}$	$h_{\text{solid}} = C_s \frac{2 K_f K_c}{K_f + K_c} \frac{P_c}{\delta^{1/2} H}$

P_{rel} = ratio of interfacial pressure to cladding Meyer hardness (approximately 680 MPa) K_m = geometric mean conductivity (W/m-K) $= 2k_f k_c / (k_f + k_c)$ $R = \sqrt{R_f^2 + R_c^2}$ (m), where R_f and R_c are the roughness of the fuel and cladding (m) $R_{mult} = 333.3 P_{rel}$, if $P_{rel} \leq 0.0087$ $R_{mult} = 2.9$, if $P_{rel} > 0.0087$ k_c = cladding thermal conductivity (W/m-K) k_f = fuel thermal conductivity (W/m-K) $E = \exp[5.738 - 0.528 \ln(3.937 \times 10^7 R_f)]$	K_f = thermal conductivity of the fuel K_c = thermal conductivity of the cladding δ = the average gas film thickness (approximated as $0.8(R_f + R_c)$) H = the Meyer hardness of the softer material $C_s = 10 \text{ m}^{1/2}$ P_c = contact pressure
--	--

The comparison conducted highlighted a few difference in the codes' method for calculating the gap conductance, in particular:

1. The code's correlation used for determining the gas thermal conductivity utilizes slightly different coefficients.
2. The approach in calculating the gap size: the total effective gap is used in the FRAPCON-4.0 model, based off the codes internal mechanics model FRACAS; BISON does not use an internal mechanics model in the gas conduction portion of its routine.
3. Method for calculating the conductance increase due to solid-to solid contact.

These differences, even if apparently minor, in calculating the gap conductance, may have an impact on the temperature difference across the gap and, subsequently, on the radial temperature profiles simulated by the codes.

8 BISON and FRAPCON-4.0 Simulation Results

Once the FRAPCON-4.0 model was developed from the BISON parameters, a simulation was performed to generate results for code comparison. The following figures show the radial temperature profile at the selected regions of the core: near the core inlet (Figure 6.4), near the center of the core (Figure 6.5), and near the core exit (Figure 6.6).

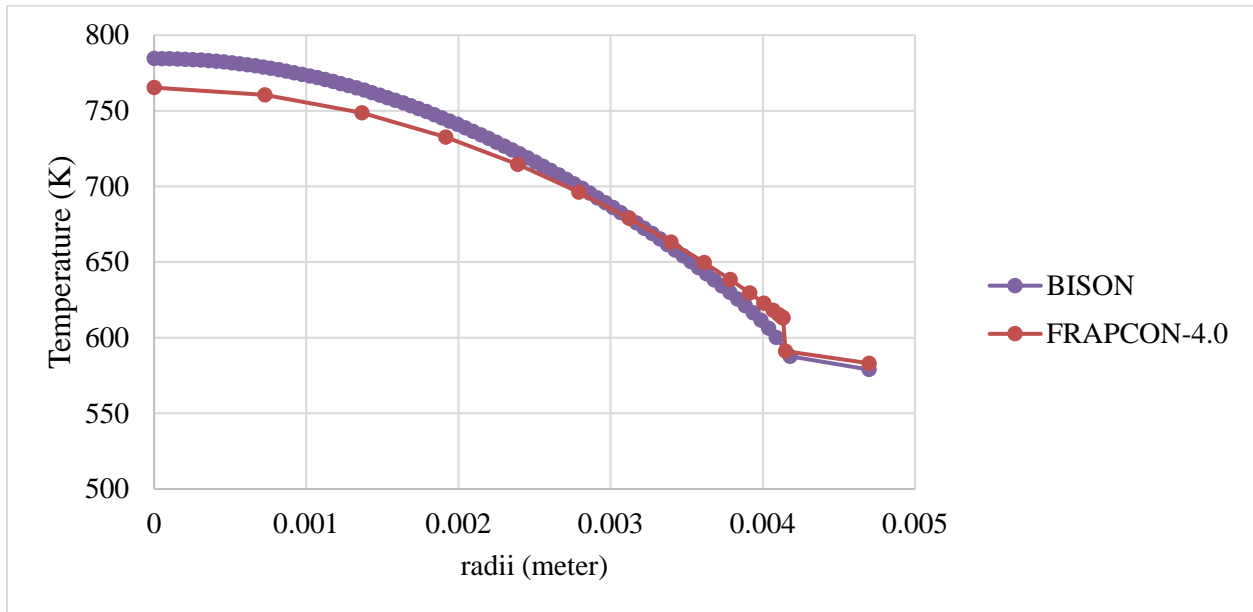


Figure 8.1: BISON and FRAPCON-4.0 model radial temperature profiles comparison near bottom of fuel pin.

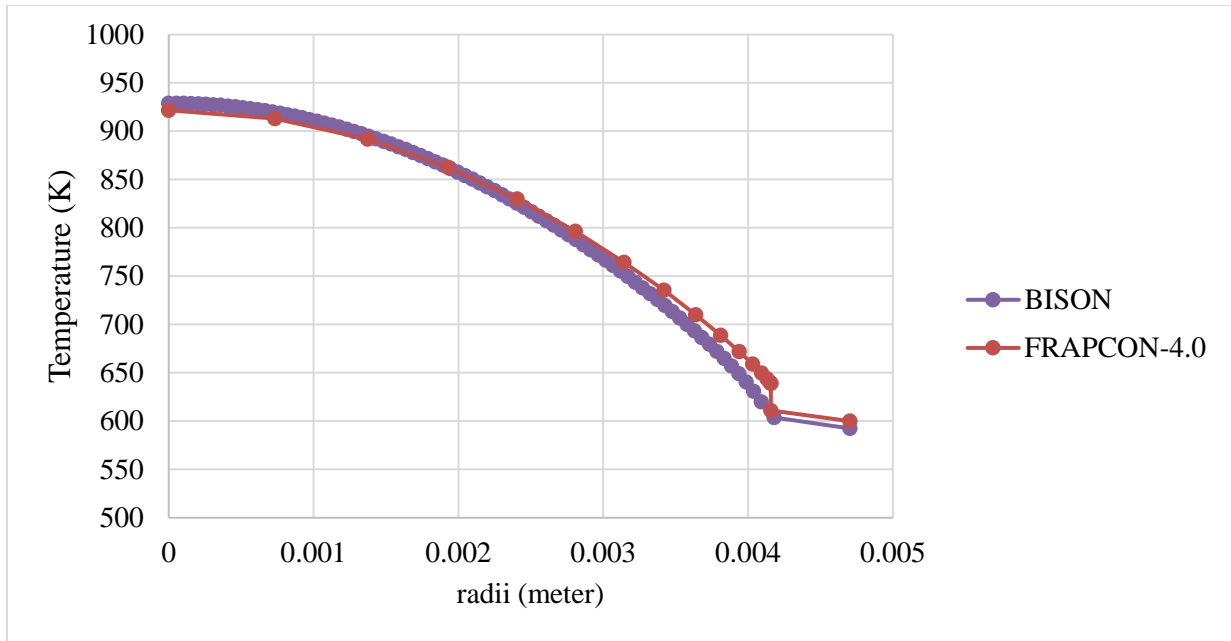


Figure 8.2: BISON and FRAPCON-4.0 model radial temperature profiles comparison in the middle of fuel pin.

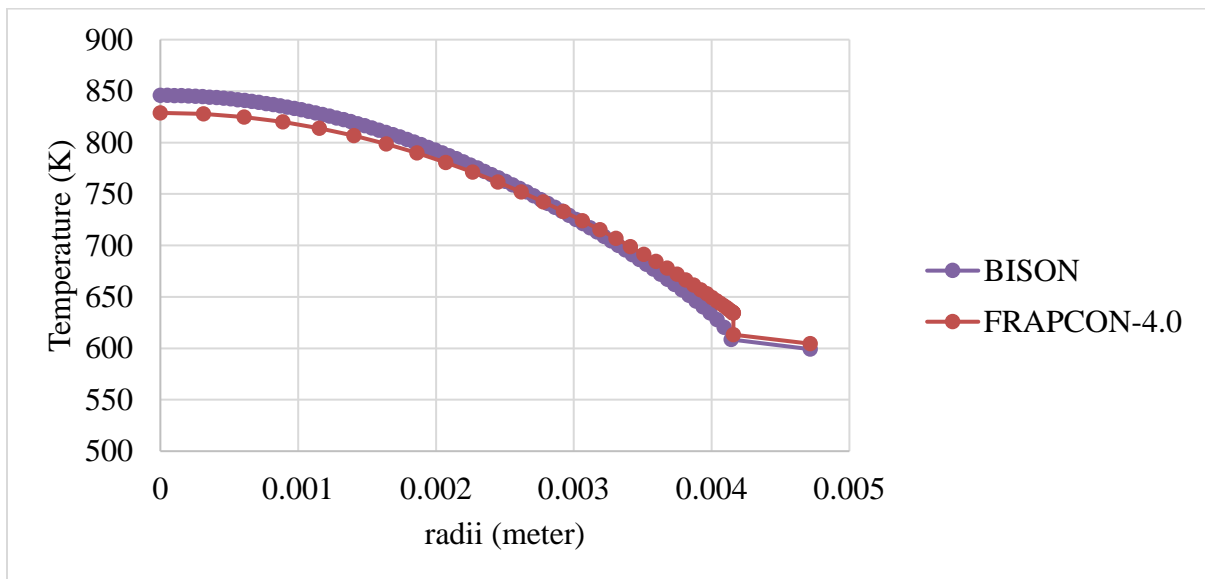


Figure 8.3: BISON and FRAPCON-4.0 model radial temperature profiles comparison near top of fuel pin.

Simulation results between the FRAPCON-4.0 model and BISON model indicate different solutions in the gap region of the radial temperature profiles. The difference in temperature gradient across the gap can be related to the difference in each codes method for calculating the gap width. Further investigation into what causes the variation in gap conductance between the codes will help determine the feasibility of using the BISON code in the LOTUS framework.

9 CONCLUSION

A literature review, code description, model development, and coupling refinements were presented along with simulation results between the fuel performance code FRAPCON-4.0 and thermal-hydraulic system code RELAP5-3D. A benchmarked exercise was also presented between the, currently used, fuel performance code FRAPCON-4.0 and, currently under development, fuel performance code BISON. This exercise also provided model descriptions and simulation results between the two code models. This work is important because it determines the feasibility of code coupling between thermal-hydraulic system codes and fuel performance codes for multi-physics transient calculations. The ability to perform these types of calculations will lead to a better understanding of the reactor system in LOCA scenarios which will aid the design and operations decisions for enhanced safety and optimization of a nuclear power plant. While performing the work presented in this thesis, the following lessons were learned.

- When performing analysis on simulation results of two different codes it is best to have geometric features matching between each code model including discretization of the nodes so the results can easily be compared for each location in the model.
- When discretization of the nodes is the same for each code model the same radial and axial power profiles should also be used, if possible, so that similar temperature profiles are expected from simulation results.
- Since RELAP5-3D does not allow radial power profiles to be supplied to every axial location, a method for supplying an averaged radial power profile to all locations has to be performed.

- RELAP5-3D can be supplied the thermal conductivity of the fuel in either a user defined temperature-dependent table or from a stored correlation in the code. The stored correlation in the system code does not take into account for burnup of the fuel so the fuel performance correlation has to be supplied to the RELAP5-3D model.
- RELAP5-3D calculates the conductance across the fuel/cladding gap using a different approach than both fuel performance codes which contributes to different temperature gradients across the gap in the radial temperature profiles when comparing simulation results.
- The approach to calculating the gap width in the gap conductance models for FRAPCON-4.0 and BISON are different which causes a difference in the temperature gradient across the gap when comparing the radial temperature profiles of each code's simulation results.
- Since the stored energy of the fuel performance simulation is the figure of merit it is important to supply the RELAP5-3D model with the time-dependent parameters at the last time step of the fuel performance model as the initial conditions for LOCA analysis.

Satisfying simulation results between the FRAPCON-4.0 model and the RELAP5-3D model encouraged the BISON and FRAPCON-4.0 simulation comparison. The result of the two code models indicated that the gap conductance differed between them. Further research into the cause of these differences can determine the possibility of obtaining similar results between the two code models. Once similar results between FRAPCON-4.0 and BISON are achieved for the same input parameters then the applicability of the BISON fuel performance code to the LOTUS framework can be determined.

REFERENCES

- [1] U. S. Nuclear Regulatory Commission, "Draft Regulatory Guide DG-1263, ADAMS Accession Number ML111100391," U.S. NRC, Washington, DC, <http://pbadupws.nrc.gov/docs/ML1111/ML111100391.pdf>, 2015.
- [2] R. Szilard, "Loss of Coolant Accident /Emergency Core Coolant System Evaluation of Risk-Informed Margins Management Strategies for a Representative Pressurized Water Reactor," Idaho National Laboratory , Idaho Falls , 2016.
- [3] W. G. Luscher, "Material Properties Correlations, Comparisons between FRAPCON-4.0, FRAPTRAN-2.0, and MATPRO," Pacific Northwest National Laboratory, Richland, WA, 2015.
- [4] R. Szilard, "Industry Application Emergency Core Cooling System Cladding Acceptance Criteria Early Demonstration, INL/EXT-15-36541," Idaho National Laboratory, Idaho Falls, 2015.
- [5] U. S. N. R. C. NRC, "Computer Codes," NRC, 04 January 2018. [Online]. Available: <https://www.nrc.gov/about-nrc/regulatory/research/safetycodes.html>. [Accessed 31 May 2018].
- [6] R.-3. D. Team, "RELAP5-3D© CODE MANUAL,VOLUME I: CODE STRUCTURE, SYSTEM MODELS, AND SOLUTION METHODS," Idaho National Laboratory, Idaho Falls, 2005 (Revision 2.3).
- [7] T. R. D. Team, "RELAP5/MOD3 Code Manual, Volumes 1 and 2," Idaho National Engineering Laboratory, Idaho Falls, August 1995.

- [8] P. O. Hikmet S. Aybar, "A review of nuclear fuel performance codes," Elsevier, Amsterdam, 2005.
- [9] C. E. B. a. K. J. G. D. D. Lanning, "Frapcon-3 updates, including mixedoxide fuel properties. Technical Report NUREG/CR-6534," PNNL-11513, Richland, WA, 2005 Vol. 4.
- [10] J. D. Hales, "BISON Theory Manual The Equations Behind Nuclear Fuel Analysis BISON Release 1.2," Idaho National Laboratory Fuel Modeling and Simulation Department, Idaho Falls, 2015 (REV.2).
- [11] W. E. Company, "Development of LWR Fuels with Enhanced Accident Tolerance," Westinghouse Electric Company LLC, Cranberry Woods, January 31, 2013.
- [12] W. G. Luscher, "Material Properties Correlations, Comparisons between FRAPCON-4.0, FRAPTRAN-2.0, and MATPRO," Pacific Northwest National Laboratory, Richland, WA, 2015.
- [13] C. M. Allison, "SCDAP/RELAP5/MOD3.1 code manual, volume IV: MATPRO-A library of materials properties for light-water-reactor accident analysis. Technical Report NUREG/CR-6150. EGG-2720,," Idaho National Engineering Laboratory, Idaho Falls, 1993.
- [14] K. O. a. N. Itagaki, "Thermal conductivity measurements of high burnup UO₂ pellet and a benchmark calculation of fuel center temperature," American Nuclear Society on Light Water Reactor Fuel Performance, page 541, Portland, Oregon, 1997.

- [15] W. L. P. R. I. P. KJ Geelhood, "A Computer Code for Calculation of Steady-State, Thermal-Mechanical Behavior of Oxide Fuel Rods for High Burnup," Pacific Northwest National Laboratory, Washington, September, 2015.
- [16] J. C. S. a. U. o. Tennessee, "Cd Doping to Reduce Reactivity of Fuel Assemblies on Spent Fuel Pools," University of Tennessee, Knoxville, 2014.
- [17] J. B. A. P. o. N. S. a. Engineering, "PWR Description," Massachusetts Institute of Technology, Cambridge, Fall 2010.
- [18] D. James J., Nuclear power : technology on trial, Ann Arbor: University of Michigan Press, 1942.
- [19] J. Fink, "Thermophysical properties of uranium dioxide," J. Nuclear Materials, Michigan, 2000.
- [20] H. J. M. a. I. J. H. P. G. Lucuta, "A pragmatic approach to modelling thermal conductivity of irradiated UO₂ fuel: review and recommendations," J. Nucl Materials, 1996.
- [21] 2. t. H. N. B. (. A. Marion (NEI) letter dated June 13, "Safety Evaluation by the Office of Nuclear Reactor Regulation of Electric Power Research Institute Topical Report TR-1002865, Topical Report on Reactivity Initiate Accidents: Bases for RIA Fuel rod Failures and Core Collabillity Criteria," NRC, Rockville, 2006.
- [22] J. D. Hales, "BISON Theory Manual The Equations Behind Nuclear Fuel Analysis BISON Release 1.2," Idaho National Laboratory Fuel Modeling and Simulation Department, Idaho Falls, 2015 (REV.2).

- [23] U. S. Nuclear Regulatory Commission, "TRACE V5.0 THEORY MANUAL, Field Equations, Solution Methods, and Physical Models," Office of Nuclear Regulatory Research, Division of Risk Assessment and Special Projects, Washington, DC, 2000.
- [24] RELAP5-3D© Development Team, "RELAP5-3D© CODE MANUAL, VOLUME I: CODE STRUCTURE, SYSTEM MODELS, AND SOLUTION METHODS," Idaho National Laboratory, Idaho Falls, 2005 (Revision 2.3).